

**KWAME NKRUMAH UNIVERSITY OF SCIENCE AND  
TECHNOLOGY KUMASI, GHANA**

**THE USE OF ELECTRICAL RESISTIVITY TOMOGRAPHY AND  
INDUCED POLARIZATION TO INVESTIGATE SEEPAGE  
CONDITIONS IN A HYDROELECTRIC DAM (A CASE STUDY OF  
THE EAST DIKE OF THE KPONG HYDRO DAM)**

**BY  
CLEMENT YIZAA DERY  
(BSC. CIVIL ENGINEERING)**

**A THESIS SUBMITTED TO THE DEPARTMENT OF GEOLOGICAL  
ENGINEERING  
(FACULTY OF CIVIL AND GEO-ENGINEERING)**

**COLLEGE OF ENGINEERING**

**IN PARTIAL FULFILMENT OF THE REQUIREMENTS FOR THE DEGREE OF**

**MASTER OF SCIENCE (GEOPHYSICAL ENGINEERING)**

**NOVEMBER,2019**

## CERTIFICATION

I hereby declare that this submission is my own work towards the award of MSc Geophysical Engineering degree and that, to the best of my knowledge, it contains no material previously published by another person, nor material which has been accepted for the award of any other degree of the University, except where due acknowledgment has been made in the text.

Dery, Yizaa Clement .....  
Signature Date

**(PG5899516, 20460113)**

Signature

Date

**Certified by:**

Dr. Frederick Owusu-Nimo. ....  
Signature Date

**(Supervisor)**

Signature

Date

Dr. Gordon Foli .....  
Signature Date

**(Head of Department)**

Signature

Date

## ABSTRACT

Earth dams are designed to permit the flow of seepage water from their reservoir through designed filter zones and relief wells. However, the flow of seepage water through other preferential flow paths either than the designed filter zones and relief wells can be detrimental to the overall stability of the dam. Conventional inspection methods such as surveillance and installation of instruments including inclinometers and settlement monuments are commonly used to detect anomalous conditions which can lead to failure on earth dams. These methods however usually detect these causes of failure after it has worsened. Geophysical techniques are non-invasive, cover a large area of the survey and are able to detect relatively small changes in physical contrast within an earth dam when used repeatedly. The ERT and IP methods were used to delineate possible seepage zones and pathways of unplanned seepage conditions that have occurred on the downstream side of the east dike of the Kpong Hydroelectric dam in Akuse, Ghana. Analysis of ERT results from the four traverse lines established along the east dike show significant anomalous conditions suggesting the existence of an unplanned seepage pathway within the lower sand and gravel overburden foundation of the dike. Very low resistivity zones ( $<25 \Omega\text{m}$ ) at different distances along the embankment was detected to be potential seepage zones. Also, the potential unplanned seepage pathway was delineated at an average elevation of 7m NDL and from 42m distance from the start of the traverse lines to 112m towards the end of the traverse lines. The IP results could not effectively detect and delineate the potential unplanned seepage zones and pathways.

# TABLE OF CONTENT

CERTIFICATION .....	ii
ABSTRACT .....	iii
TABLE OF CONTENT .....	iv
LIST OF TABLES .....	vii
LIST OF FIGURES .....	viii
LIST OF PLATES .....	ix
LIST OF ABBREVIATIONS .....	x
ACKNOWLEDGMENT .....	xi
<b>CHAPTER ONE</b> .....	<b>1</b>
<b>INTRODUCTION</b> .....	<b>1</b>
1.1 Background of the Study.....	1
1.2 Problem Statement .....	2
1.3 Objectives of the Research.....	2
1.4 The significance of the Study.....	3
1.5 Scope of Work .....	3
1.6 The organization of the Study.....	3
<b>CHAPTER TWO</b> .....	<b>3</b>
<b>LITERATURE REVIEW</b> .....	<b>3</b>
2.1 Dams and classifications .....	3
2.2 Earth Embankment Dams .....	4
2.2.1 Zoned Earth Embankment Dams .....	5
2.2.2 Materials for Earth Embankment Dams.....	8
2.2.2.1 Fine-grained Soil.....	8
2.2.2.2 Coarse-grained soil .....	8
2.2.2.3 Coarse rockfill and boulders .....	9
2.2.3 Common Failure Modes in Earth Dams .....	9
2.2.3.1 Earth Dam failure by internal erosion/piping .....	9
2.2.3.2 Earth Dam failure by overtopping .....	9

2.2.3.3 Structural failure of Earth Dams .....	9
2.2.4 Monitoring in Earth Embankment Dams .....	10
2.3 Theory of permeability and flow through geomaterials.....	10
2.3.1 Darcy’s Theory of flow.....	11
2.3.2 Flow Nets .....	12
2.3.3 Phreatic Line .....	13
2.4 Geophysical Techniques .....	14
2.4.1 Electrical Resistivity .....	14
2.4.1.1 Theory and Basic Principle of Electrical Resistivity .....	15
2.4.1.2 Apparent Resistivity and True Resistivity .....	19
2.4.2 Induced Polarization .....	19
2.4.3 The ABEM Terrameter .....	21
2.5 Application of Geophysical Techniques to Investigate Seepage Conditions in Earth Dams .....	22
<b>CHAPTER THREE .....</b>	<b>25</b>
<b>BACKGROUND OF THE KPONG HYDROELECTRIC DAM .....</b>	<b>25</b>
3.1 Site Location and Setting of the Kpong Hydroelectric Dams and Dikes.....	25
3.2 Bedrock of Kpong Hydroelectric Dam .....	27
3.3 Overburden Material of East Dike .....	27
3.4 Composition of the Kpong East Dike .....	28
3.5 Location of Unplanned Seepage Points .....	30
<b>CHAPTER FOUR.....</b>	<b>31</b>
<b>METHODOLOGY.....</b>	<b>31</b>
4.1 Survey Plan .....	31
4.2 Resistivity and Induced Polarization Measurement.....	33
4.3 Data Processing.....	34
<b>CHAPTER FIVE.....</b>	<b>34</b>
<b>RESULTS AND DISCUSSION .....</b>	<b>34</b>
5.1 Results of Electrical Resistivity Tomography of the Study Section of the East Dike .....	34
5.2 Results of Induced Polarization (IP) Survey of the Study Section of the East Dike .....	40
5.3 Delineation of potential seepage pathway .....	43
<b>CHAPTER SIX .....</b>	<b>45</b>
<b>CONCLUSION AND RECOMMENDATION .....</b>	<b>45</b>
6.1 Conclusion .....	45

6.2 Recommendation ..... 46

**REFERENCES**..... 46

**APPENDICES** ..... 49

Appendix A Edited data for 50 data points for Resistivity and Chargeability ..... 49

Appendix B Software Used..... 58

Appendix C Overburden soil stratigraphy of East Dike ..... 59

KNUST



## LIST OF TABLES

Table 2.1 USCS classification of fine-grained soils .....	8
Table 4.1 Coordinate of survey locations .....	32
Table 5.1 Respective distance of Relief Wells .....	39

# KNUST



## LIST OF FIGURES

Figure 2.1 Typical earth embankment dike .....	6
Figure 2.2 Flow of water through soil medium .....	12
Figure 2.3 Construction of flow nets in an earth dam .....	13
Figure 2. 4 Homogeneous dam showing phreatic surface .....	14
Figure 2.5 Cylindrical body .....	16
Figure 2.6 Single point current flow through a homogeneous isotropic subsurface .....	17
Figure 2.7 Flow of current from the source and sink through a subsurface .....	17
Figure 2.8 Arrangement of current and potential electrodes .....	18
Figure 2.9 Basic theory for current flow with respect to time .....	20
Figure 2.10 Geoelectrical imaging system with Terrameter LS .....	21
Figure 3.1 Location of Kpong Hydroelectric Dam with respect to Ghana .....	26
Figure 3.2 Kpong Hydroelectric Dam .....	26
Figure 3.3 Typical partial cut-off section of the East Dike .....	29
Figure 3.4 Detail representation of dike in the study section. ....	30
Figure 3.5 Overburden stratigraphy of the East Dike showing study section .....	30
Figure 4.1 Orientation of traverse lines .....	33
Figure 5.1 Traverse Line 1 Resistivity Pseudosection .....	36
Figure 5.2 Traverse Line 2 Resistivity Pseudosection .....	37
Figure 5.3 Traverse Line 3 Resistivity Pseudosection .....	38
Figure 5.4 Google view of Relief Wells positions .....	39
Figure 5.5 Graph of relief wells against measured seepage water level for 2018 .....	40
Figure 5.6 Possible siltation of relief well .....	40
Figure 5.7 Traverse Line 4 Resistivity Pseudosection .....	41
Figure 5.8 Traverse Line 1 Induced Polarization Pseudosection .....	42
Figure 5.10 Traverse Line 3 Induced Polarization Pseudosection .....	43
Figure 5.11 Traverse Line 4 Induced Polarization Pseudosection .....	44
Figure 5.12 (a) Possible delineated unplanned seepage pathway from resistivity results combined (b) A sectional view of the delineated unplanned seepage pathway from resistivity results .....	46

## LIST OF PLATES

- Plate 3. 1 Unplanned seepage location ( $6^{\circ}8'28.00''N$  latitude and  $0^{\circ} 7'39.98''E$  longitude) .... 31
- Plate 4.1 Measurement of resistivity and induced polarization in progress ..... 34

# KNUST



## LIST OF ABBREVIATIONS



<i>2D</i>	2 Dimension
<i>A</i>	Cross-sectional Area
<i>AC</i>	Alternative Current
<i>BC</i>	Before Christ
<i>DC</i>	Direct Current
<i>E</i>	East
<i>El</i>	Elevation
<i>ERT</i>	Electrical Resistivity Tomography
<i>GPR</i>	Ground Penetration Radar
<i>GPS</i>	Global Positioning System
<i>I</i>	Current
<i>ICOLD</i>	International Commission on Large Dams
<i>IP</i>	Induced Polarization
<i>J</i>	Current Density
<i>K</i>	Geometric Factor
<i>L</i>	Length
<i>N</i>	North
<i>NDL</i>	National Datum Level
$\rho$	Resistivity
$\rho_a$	Apparent Resistivity
<i>r</i>	Radial Distance
<i>R</i>	Resistance
<i>RQD</i>	Rock Quality Designation
<i>RW</i>	Relief Well
<i>SP</i>	Self Potential
<i>USSD</i>	United States Society on Dams
<i>USCS</i>	Unified Soil Classification System
<i>V</i>	Voltage
<i>VRT</i>	Vertical Resistivity Tomography

## ACKNOWLEDGMENT

I would like to express my deepest appreciation to me by my Supervisor Dr. Owusu-Nimo, who gave me the opportunity to undertake this research work in his office. I acknowledge the crucial role he played to ensure the successful completion of my research.

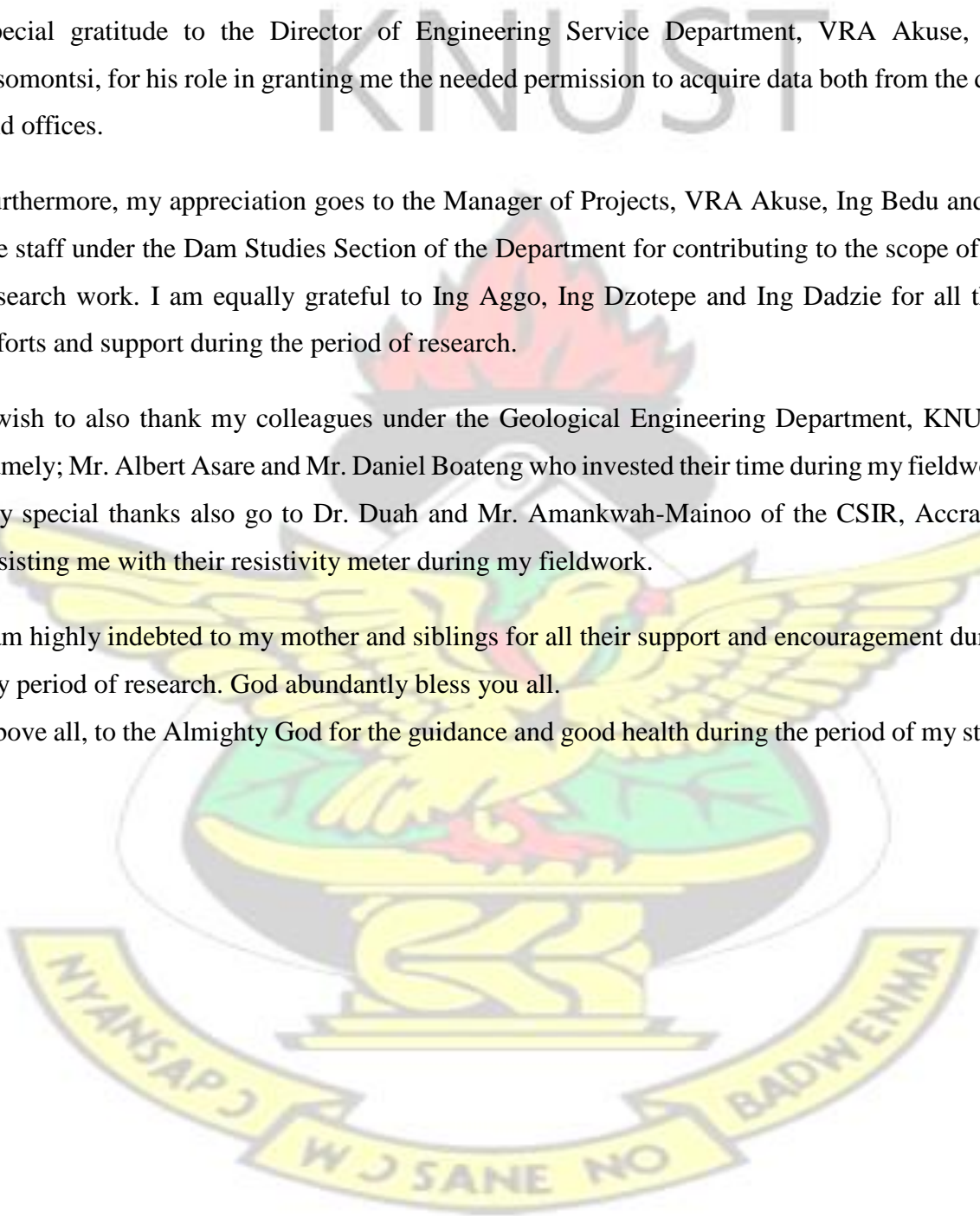
Special gratitude to the Director of Engineering Service Department, VRA Akuse, Ing Asomonsi, for his role in granting me the needed permission to acquire data both from the dam and offices.

Furthermore, my appreciation goes to the Manager of Projects, VRA Akuse, Ing Bedu and all the staff under the Dam Studies Section of the Department for contributing to the scope of my research work. I am equally grateful to Ing Aggo, Ing Dzotepe and Ing Dadzie for all their efforts and support during the period of research.

I wish to also thank my colleagues under the Geological Engineering Department, KNUST, namely; Mr. Albert Asare and Mr. Daniel Boateng who invested their time during my fieldwork. My special thanks also go to Dr. Duah and Mr. Amankwah-Mainoo of the CSIR, Accra for assisting me with their resistivity meter during my fieldwork.

I am highly indebted to my mother and siblings for all their support and encouragement during my period of research. God abundantly bless you all.

Above all, to the Almighty God for the guidance and good health during the period of my study



# CHAPTER ONE

## INTRODUCTION

### 1.1 Background of the Study

A dam is any structure constructed to hold water behind it for purposes of irrigation, domestic and commercial water supply, hydroelectric power generation, flood control, and recreation. Dams have been grouped into various classes by different people and institutions. For example, the United States Society on Dams classify dams into Gravity, Arch, Buttress, Cofferdam, Diversion, Embankment, Hydropower, Industrial Waste Dam, Masonry, Overflow, Regulating and Saddle Dams. Dams have also been classified based on function, construction material, and structural design. Murthy et al. (2015), however, classify dams into two broad categories; embankment and concrete dams. While embankment dams consist of layers of compacted suitable earth or crush rock materials to serve as a water barrier, concrete dams (also called masonry dams) consist of concrete, reinforced concrete, rocks or bricks laid together to act as a water barrier.

Embankment dams have been reported to be the most predominant dams worldwide aside being one of the earlier dams ever constructed. Report from the international commission on large dams (ICOLD), in 2018, indicates that out of the 14,000 large dams registered by the body, 70% of them are embankment dams. Embankment dams, like any hydraulic structure, can fail if not operated well. One of the commonest modes of failure in embankment dams is piping.

In designing embankment dams, planned seepage is allowed with the provision of designed filter zones and relief wells (Lin et al., 2013). However, preferential flow paths can develop through the embankment or its foundation, thereby causing unplanned seepage conditions which can lead to dam failure.

Embankment dams are therefore usually monitored for unplanned seepages and defects using conventional methods such as visual inspection and surveillance, drilling, and other instrumentation methods such as piezometers, inclinometers and relief wells (Johansson, 1997).

## **1.2 Problem Statement**

The Kpong Dam is a Hydroelectric Dam owned and operated by the Volta River Authority in Ghana. The dam can be classified as a zoned embankment dam. It was designed and constructed with three different materials namely; silty clay core, sand filter, fine and coarse rock fill.

An unplanned seepage, which can be described as water exiting as a boil, has been discovered along the toe drain of the east dike of the dam. This unplanned seepage condition was initially witnessed in small volumes in the 1980s after the dam was completed. However, special attention was drawn to the location in 2017 after the seepage condition worsened with the flow of large volumes of water when a weir was constructed around the unplanned seepage zone to measure the flow rate.

In January 2017, several excavations were carried out around the unplanned seepage point to trace the possible pathway for the unplanned seepage point which was unsuccessful. Therefore, french drains were constructed within the vicinity of the unplanned seepage point to be used as a medium of trapping and disposing of the seepage water which was also unsuccessful after the drains failed to trap any seepage water.

This study, therefore, explores the possibility of using geophysical techniques to detect and delineate the seepage zones and possible unplanned pathways on the east dike of the dam.

## **1.3 Objectives of the Research**

The general objective of the study is to use the Electrical Resistivity Tomography and the Induced Polarization method to investigate the seepage conditions at the East dike of the Kpong Hydroelectric Dam. To achieve this goal the research intends:

- To assess the possibility of using the electrical resistivity tomography (ERT) in delineating possible seepage zones and pathways in the Kpong Hydroelectric Dam
- To assess the possibility of using the induced polarization (IP) method in delineating possible seepage zones and pathways in the Kpong Hydroelectric Dam.
- To detect and delineate possible seepage pathways within the dam using a combination of geophysical methods.

#### **1.4 The significance of the Study**

The early detection and delineation of possible seepage zones within an earth dam are very cardinal to ensuring the integrity of such dams. Being able to use geophysical methods for such investigation will be very ideal because of its non-invasiveness and its ability to give large-scale information quickly and cost-effectively. The results from the study will provide the seepage conditions and possible flow paths within the East Dike of the Kpong Dam to enable remediation measures to be carried out. This study will also provide a means of using geophysical techniques in assessing seepage conditions of earth dams in Ghana for early detection of any unplanned seepages to prevent any catastrophic failure.

#### **1.5 Scope of Work**

The geophysical technique adopted for this study includes Electrical Resistivity and Induced Polarization methods. The results presented in this study was based on four (4) traverse lines conducted on the East Dike of the Kpong Dam between chainage 5km+385m to 5km+625m and other geotechnical design information from the geotechnical completion report of the Kpong Hydroelectric Dam.

#### **1.6 The organization of the Study**

Chapter one gives a brief introduction to the study including the scope and the problem statement. Chapter two reviews the literature on various earth embankment dams, common failure methods, monitoring techniques including non-destructive methods and the theory of permeability and seepage through geomaterials. Chapter three discusses the location and setting of the Kpong Hydroelectric Dam and the bedrock condition of the study area. Also, the overburden and composition of the east dike are presented in this chapter. Chapter four presents the materials and methods used in obtaining the data and the results that were obtained are discussed, analyzed and interpreted in Chapter five. Chapter six outlines the conclusions and recommendations that were successfully drawn from the study.

## **CHAPTER TWO**

### **LITERATURE REVIEW**

#### **2.1 Dams and classifications**

A dam is any barrier built to impound water, wastewater, or any liquid-borne material, for the purpose of storage or control of water. Dams are made with either earth material, stacked rock

or concrete and constructed across rivers to store water in the reservoir that accumulates behind the dam as the result of the blockage of the river.

There are several classifications of dams by different organizations and authors. Some notable classifications include the United States Society on Dams (USSD), which classify dams into gravity, arch, buttress, coffer, diversion, embankment, hydropower, industrial waste dam, masonry, overflow, regulating and saddle dams. The international commission on large dams (ICOLD) on their website in 2018, also classifies dams according to; type, spillway, reservoir capacity, irrigated area, etc. Also, all dams in torrential watersheds have been classified based on the construction types and include functional purposes, the shape of the functional part of the dam, the building material and the static system (Wehrmann, et al., 2006). Dams have been broadly grouped based on hydraulic design, example are overflow, non-overflow, rigid, non-rigid dams and based on their purpose such as storage, diversion, detention, debris, cofferdams (Bhattarai et al., 2016). Again, Murthy et al. (2015) broadly classify dams into two, namely: embankment and concrete dams. Embankment dams are earth-filled or rockfill while concrete dams are made of concrete. Finally, the Bureau of Reclamation (2011) has further classified embankment dams based on the kind of material used for filling the embankment. These include earth and rockfill embankment materials. While the earth-dams consist of suitable soils obtained from borrow pits, the rock-filled dam is composed of fragmented rock with an impervious core.

## **2.2 Earth Embankment Dams**

Embankment dams are constructed of natural materials such as earth or fine rock that rely on its weight and various material characteristics to control seepage for its stability (New Hampshire Department of Environmental Services, 2011). Rajeeth(2011) reports that there are 30,000 earth dams recorded worldwide with heights of more than 15m with more than half of them constructed since 1950. Earth embankment dams continue to be the most predominate dams worldwide because its construction involves the use of borrow materials that are readily available on or close to the site.

Earth embankment dams have been put into three groups based on the type of materials and location of the material within the embankment (Bureau of Reclamation, 2011). These include homogeneous, diaphragm and zone embankment earth dams.

A homogenous dam is constructed of a single kind of impervious material (Aboelela, 2016). With this type of dams, excess pore pressures can build up within the embankment, especially with dams having fluctuating water levels or dams having impervious foundations.

The diaphragm type of dams has the bulk of its embankment constructed of pervious materials such as sand, gravel or crush rock. A thin membrane called the diaphragm which is constructed of either concrete, metal, asphaltic concrete and compacted earth is placed either near the upstream end or the mid-portion of the embankment to serve as a water barrier. This kind of dam can be deficient in functions due to the non-availability of the diaphragm for inspection and repair (Bureau of Reclamation, 2011).

Zoned embankment dams take advantage of the availability of different types of earth materials by placing these materials in various zones within the embankment. By so doing the materials complement one another to reduce seepages. The various zones in this type of dam are divided into three, namely: the pervious for the downstream section, the impervious for the core or midsection and the semi-pervious for the upstream side.

### **2.2.1 Zoned Earth Embankment Dams**

This type of earth embankment dam has three main categories of earthworks mainly; the pervious for the downstream section, the impervious for the core and the semi-impervious for the upstream section of the dam or dike. According to Johansson (1997), the central portion of the dam called the core consist of a material of low permeability such as moraine. The filter or casing which surrounds the core is semi-permeable compared to the core and prevents the washout of the fine core material. Finally, the fill material located at the periphery of the embankment is usually made up of gravel or rock fill and its purpose is to stabilize the dam by transferring the water load to the ground.

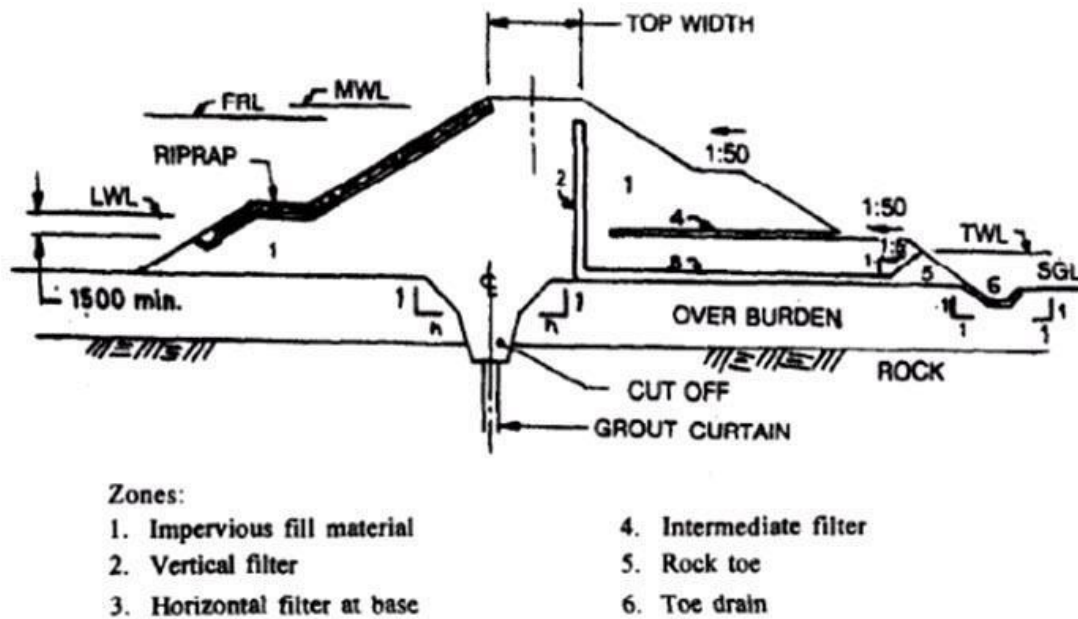


**Figure 2.1 Typical earth embankment dike**

Some basic terminologies used in earth dams are explained below:

- **BASE WIDTH:** The width of the dam measured along the dam/foundation interface.
- **BERM:** A berm is a level space along an embankment usually made of compacted soil and separating two different level areas.
- **BREACH:** An opening in the dam mostly caused by excessive erosion of the embankment
- **CONDUIT:** Any pipe or closed channel constructed to discharge water through or under a dam.
- **CORE:** Is the impervious zone of material in the embankment fill which has low permeability.
- **CREST LENGTH:** This length can be said to be the total length of the dam.
- **CREST OF THE DAM:** Is simply the topmost portion of the embankment surface. It can also be termed the overflow section.
- **CUTOFF WALL:** A wall of impervious material, e.g., concrete, wood pilings, steel sheet piling, built into the foundation to reduce seepage under the dam.
- **CUTOFF:** An impervious construction by means of which seepage is reduced or prevented from passing through foundation material.
- **CUTOFF:** Is an impervious section constructed at the foundation of the dam to reduce seepage or prevent water from passing through its foundation

- **DRAINAGE LAYER OR BLANKET:** This pervious material is used to facilitate seepage by constructing it directly over the foundation material or downstream slope.
- **DRAWDOWN:** The resultant lowering of water level due to the loss of water from the reservoir.
- **EMBANKMENT:** Any Fill material, usually earth or rock, placed with sloping sides.
- **FACE:** With reference to a structure, the external surface that limits the structure, e.g., the face of the wall or dam
- **FILL:** Granular materials such as crush rock placed on the periphery of the dam to receive the load from the wave and transmit it to the ground safely.
- **FILTER:** Any semi-pervious material placed on top of the core material.
- **FOUNDATION OF DAM:** The natural material on which the dam structure is placed.
- **FREEBOARD:** The vertical distance between the water surface and the lowest part of the dam crest.
- **INTAKE:** Any structure in a reservoir, dam, or river through which water can be drawn into an outlet pipe, etc.
- **PERVIOUS ZONE:** This zone is also called the filter. The materials here are highly permeable compared to the core.
- **RELIEF WELL:** Vertical pipes in downstream of an embankment dam to collect and control seepage through or under the dam and so reduce water pressure.
- **RIPRAP:** These are crush rocks placed in a random manner on the upstream slope of the embankment to protect it against the actions of waves.
- **SEEPAGE COLLAR:** Is the projecting collar usually constructed of concrete or steel built around the outside of a pipe, tunnel, or conduit, under an embankment dam, to lengthen the seepage path along the outer surface of the conduit.
- **SPILLWAY:** This is a structure used to provide the controlled release of flows from a dam or levee into a downstream area, typically the riverbed of the dammed river itself.
- **STRUCTURAL HEIGHT:** The vertical distance from the lowest point of natural ground on the downstream side of the dam to the highest part of the dam which would impound water.

- TOE OF DAM: The junction of the downstream face of a dam with the natural ground surface.
- TOP OF DAM: The elevation of the uppermost surface of a dam, usually a road or walkway, excluding any parapet wall, railings, etc.

### 2.2.2 Materials for Earth Embankment Dams

With the exception of organic soils and peat, all geological materials are used for the construction of earth embankment dams. Most earth embankment dams are economically designed to utilize the bulk of its materials from nearby borrow pits. These materials range from both fine and coarse-grained soils to crushed rock for the periphery of the dam.

The classes of materials mostly used are explained in the sections below.

#### 2.2.2.1 Fine-grained Soil

Clays and silts usually fall under this group of soil and often are used in homogenous dams and in the impervious sections of zoned embankment dams (United States Society on Dams Materials, 1985). By USCS definition, fine-grained soils are soils with 50% or more of their total weight have sizes smaller than 75 micron IS sieve size. Clay and silt, however, exhibit different characteristics in terms of strength, compressibility, and permeability. They also have different sieve sizes. According to USCS, the various size distribution for clay and silt are as follows:

**Table 2.1 USCS classification of fine-grained soils**

1	Silt	0.002mm-0.075mm
2	Clay	<0.002mm

#### 2.2.2.2 Coarse-grained soil

Coarse-grained soil by USCS can be divided into gravel and sand. For gravel materials, 50% of the coarse fractions are larger than 4.75mm sieve size. Also, 50% of the coarse fractions in sandy soil are smaller than 4.75mm sieve size. Coarse-grained soils such as sand are used in filter zones in zoned embankment dams. Gravelly materials are mostly used as fill in zones of embankment dams especially that of zoned embankments.

### **2.2.2.3 Coarse rockfill and boulders**

Coarse rock between 60mm to 200mm and over 200mm for boulders of recommended competence is usually placed along the periphery especially at the upstream side of an earth embankment dam to receive and safely transmit the pressure of the water waves to the ground.

## **2.2.3 Common Failure Modes in Earth Dams**

### **2.2.3.1 Earth Dam failure by internal erosion/piping**

There is a variation between internal erosion and piping. While internal erosion occurs within the embankment, piping can occur both within the embankment and under or through the foundations of the embankment. In both cases, either of them can lead to failure. Internal erosion usually occurs when water flows through cavities or cracks within the embankment (Hanson et al., 2010). These cavities can be caused by mechanical or chemical means. Also, poor construction or materials can lead to the creation of voids within an embankment resulting in internal erosion. Internal erosion has been reported by ICOLD to cause about 46% of dams failure among large dams registered between 1800 and 1986 excluding dams in Japan (pre-1930) and China (ICOLD, 2013).

Piping is the erosion of soil material due to foundation or embankment seepage (Blackett, 2013). Piping is caused by an imbalance in macroscopic soil stresses and pore water pressure (Carlsten et al., 1995). The US Department of the Interior Bureau of Reclamation (2015) has described piping as a specific type of internal erosion.

### **2.2.3.2 Earth Dam failure by overtopping**

Overtopping occurs when the flood outlet cannot release the water fast enough and the water rises above the dam and spills over (Goodarzi et al., 2012). Overtopping has been described as a form of hydraulic failure (New Hampshire Department of Environmental Services, 2011). It is the unplanned flow of water over the embankment and can be caused by high levels of water in the reservoir. According to ICOLD (2013) overtopping is a form of erosion termed external erosion which accounts for about 48% of earth dam failure among large dams registered between 1800 and 1986 excluding dams in Japan (pre-1930) and China. Also, according to Wehrmann and Johannes (2006), one-third or more of the total identified failure of embankment dams was caused by overtopping.

### **2.2.3.3 Structural failure of Earth Dams**

This condition can be caused by the separation of the embankment materials and its foundation or shear failure causing slide along the slopes. Excessive loading or natural disasters can also

cause embankment dams to shear or settle unevenly. Sloughs, cracks, and bulges in the embankment or dike are some signs of serious instability and may lead to structural failure. About 25% of earth dams failure is attributed to structural failures (Kirra et al., 2015).

#### **2.2.4 Monitoring in Earth Embankment Dams**

One essential part of the life of a dam is the continued monitoring of the dam for performance. This commonly takes a form of visual inspection around the dam and its dikes. Several embankment dams come with the installation of instrumentation to complement the inspection process. This instrumentation is usually installed during construction and includes piezometer, inclinometers, relief wells and settlement monuments. The observation/inspection methods and the monitoring instruments can, therefore, be classified as monitoring devices. There are several classifications to dam monitoring. Johansson (1997) classified the new ways of dam monitoring as built-in monitoring, borehole methods, non-destructive testing methods, and other methods.

Built-in monitoring methods which include instrumentation like inclinometer, monuments, relief wells, and piezometer are built during the construction of the dam. Inclinometers and monuments provide information on the movement of the dam embankment and the dikes. Relief wells and piezometers respectively measure the seepages and pressure of the reservoir water. These data when acquired can give useful information on the integrity of the dam. Also, pressure measurement, infiltration and temperature readings can be obtained by drilling to install standpipes on the dam or dikes.

Finally, a non-invasive method of earth dam monitoring is available. Geophysical techniques rely on the variation in material properties to predict changes in the subsurface conditions of the soil. Electrical Resistivity Tomography (ERT), Self-Potential (SP), Induced Polarization (IP), Seismic Refraction and the Ground Penetration Radar (GPR) methods are commonly used in monitoring changes in a dam. This method of monitoring has the advantage of detecting relatively small changes in the embankment when used repeatedly.

#### **2.3 Theory of permeability and flow through geomaterials**

Permeability in soil materials is simply the measure of the ability of the material to permit the flow of fluid through it. The permeability of any soil material is dependent on the degree of porosity and also the tortuosity of the pore spaces within the soil material. A high porous and tortoise materials result in a more permeable soil medium. An example of a pervious material is gravel while clay material is an impervious material. The understanding of permeability in soil medium is an essential tool in determining seepage through and below earth structures,

determination of uplift pressure of hydraulic structures, and settlement of structures. The principle of flow of fluid through a porous medium is governed by Darcy's Law.

### 2.3.1 Darcy's Theory of flow

Darcy's Law is an equation that describes the flow of fluid through a porous medium. The law is a simple proportional relationship between the instantaneous discharge rate through a porous medium, the viscosity of the fluid and the pressure drop over a specified distance (Kiplangat Vincent et al., 2014).

For a laminar flow through a saturated soil medium, the rate of discharge per unit time is proportional to the hydraulic gradient.

$$q = KiA \tag{Equation 2.1}$$

$$\frac{q}{A} = Ki$$

But  $V = \frac{q}{A}$

Therefore,  $V = Ki$  (Equation 2.2)

Where  $q$  is the discharge per unit time (rate of flow),  $A$  is the total area of the soil medium,  $i$  is the hydraulic gradient which can be expressed as  $\frac{h}{L}$ . Also,  $K$  is Darcy's coefficient of permeability, while  $V$  is the velocity of flow (discharge velocity)

If a soil sample of cross-sectional area  $A$  and length  $L$ , is subjected to a differential head of flow, the hydraulic gradient  $i$  is given by;

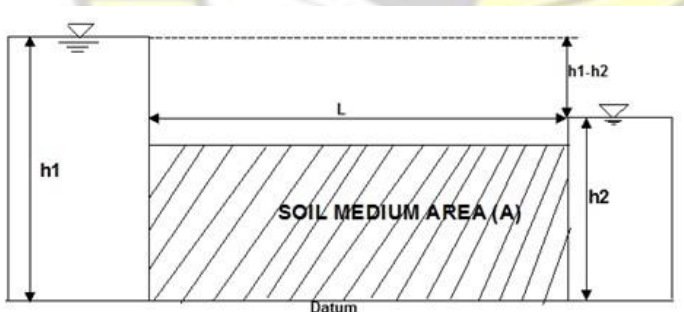


**Figure 2.2 Flow of water through soil medium**

$$h = \frac{h_1 - h_2}{L}$$

$$i = \frac{h_1 - h_2}{L} \quad \text{(Equation 2.3)}$$

But from equation 2.1;

$$q = (-)K \frac{h_1 - h_2}{L} * A \quad \text{(Equation 2.4)}$$

The negative sign in the equation shows that the velocity of flow occurs in the direction of decreasing head.

Earth dams are usually constructed over a soil medium with some degree of porosity and saturation. Depending on the porosity and saturation of the underlying material of the dam, water may be forced to percolate into it due to the pressure difference (hydraulic gradient) between the reservoir and the unsaturated soil medium. This process can lead to seepage of water through paths of least resistance within the soil mass.

Darcy's law can be used to estimate the rate of flow, the flow velocity, and the total discharge through an earth dam.

### 2.3.2 Flow Nets

Flow net is a graphical representation of how water flows through a soil mass. It is a combination of flow lines and equipotential lines to form a curvilinear net. While a flow line is a path for which water particles follows in the course seepage, equipotential lines are formed by joining points of the same head or potentials on a flow line. Flow nets are used in solving groundwater flow through, for instance, a dam where the geometry of flow is complicated. Flow nets can be used to determine the rate of flow and seepage pressure for a given soil mass of an earth dam. A successful seepage analysis of an earth dam is achieved on the proper and accurate construction of flow nets (Sachpazis, 2014). Seepage is the continues movement of water from the upstream face of a dam towards its downstream face (Moayed et al., 2012). Seepage water migration across an earth dams depends on the permeability and hydraulic gradient between the reservoir and the downstream of the dam.

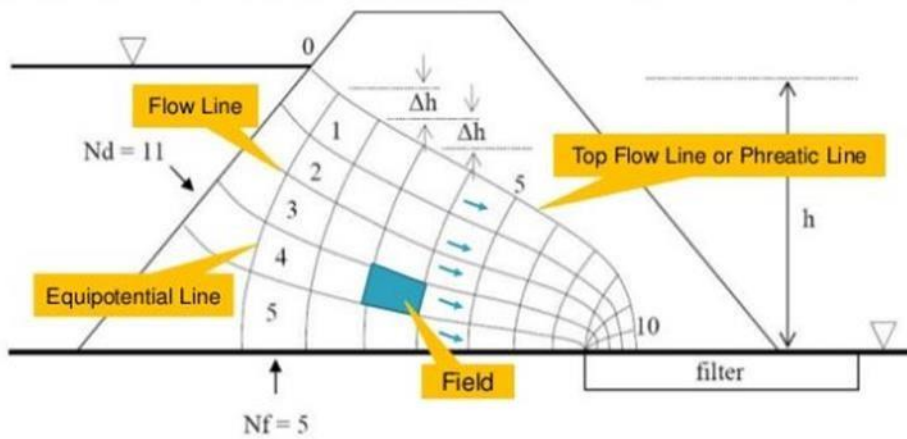


**Figure 2.3 Construction of flow nets in an earth dam**

1. For a given soil medium the discharge can be determined using the following equation;

$$q = K * H * \frac{N^f}{N_d} \quad \text{(Equation 2.5)}$$

Where  $q$  is the discharge,  $H$  is the head causing the flow,  $N_d$  is the number of flow channels and  $N^f$  is the number of potential drops.

2. The change in effective pressure due to the flow of seepage water is known as seepage pressure. The seepage pressure can be determined using;

$$P_s = \gamma_w * h = \gamma_w(H - n * \Delta h) \quad \text{(Equation 2.6)}$$

Where  $P_s$  is the seepage pressure,  $\gamma_w$  is the unit weight of water,  $h$  is the total head, and  $\Delta h$  is the change in head.

### 2.3.3 Phreatic Line

It is defined as an imaginary line within the dam section, below which there is positive hydrostatic pressure, and above there is negative hydrostatic pressure in the dam section. Below the phreatic line is a saturated portion where seepage takes place while above the phreatic line is the unsaturated portion of the dam. The slope of a phreatic line is thought to be the direction of the flow of water in a dam or an aquifer. The phreatic line can be a flow line within a flow net.

In designing an earth dam section, the phreatic line plays an important role because the safety of the dam depends on it. The fluctuations of water level in dams can induce changes in the phreatic line or pore water pressure in the waterfront of slopes in earth dams which can contribute to failure (Yan et al., 2010). Therefore calculating the phreatic line or pore water

pressure in the waterfront slope of an earth dam is very useful in the analyzation of slope stability.

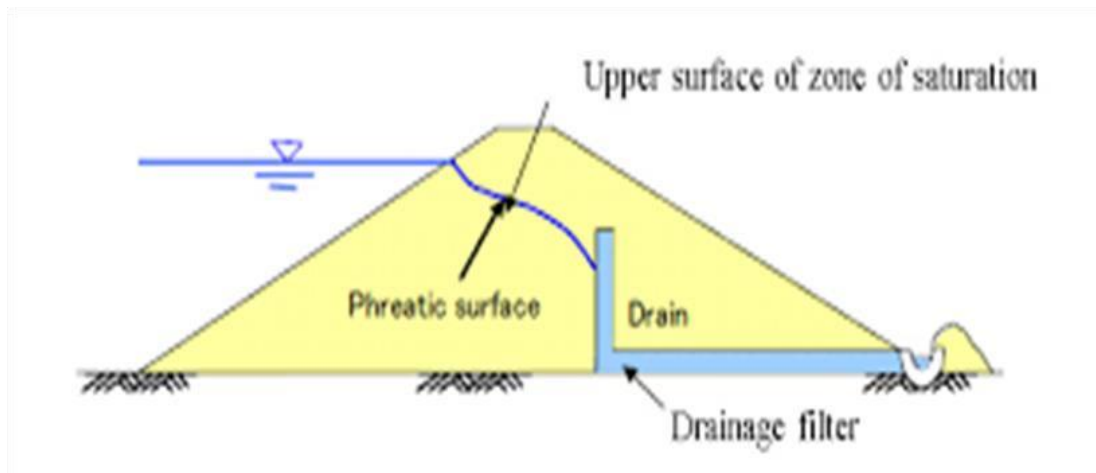


**Figure 2. 4 Homogeneous dam showing phreatic surface**

## 2.4 Geophysical Techniques

Geophysical methods of investigation entail the measurement of mediums associated with changes in the physical properties such as density, magnetic susceptibility, electrical conductivity, and elasticity in the near or subsurface of the earth (Herman, 2001). The changes in these physical properties mark some anomalies in the subsurface of the earth. Data obtained from this measurement can be processed to obtain an estimate of the depth, size or competence of any physical property near or under the subsurface of the earth. There are both passive- and active-source techniques for data acquisition.

Some of the widely used methods include electrical resistivity, induced polarization, selfpotential, seismic reflection/refraction, electromagnetic methods, and ground penetration radar techniques.

### 2.4.1 Electrical Resistivity

The electrical resistivity of a material is the measure of how well the material retards the flow of electrical current (Herman, 2001). This is expressed in Ohm-meters ( $\Omega\text{m}$ ). Electrical resistivity can also be explained to be the measurement of apparent resistivity of soils or rock as a function of depth. The bulk average resistivity of any soil or rock material within the subsurface influencing the flow of current is called the apparent resistivity,  $\rho_a$ . It is calculated by dividing the potential difference  $V$  of the subsurface by the injected current  $I$  and multiplying by the geometric factor  $K$  specific to the array being used and the electrode spacing.

$$\rho_a = K \frac{AV}{I}$$

(Equation 2.7)

Where Unit for Voltage(V) is volts(V), Current(I) as amperes(A) with **K** as a dimensionless constant. The resistivity of any soil or rock materials is related to some geological parameters which include the porosity, permeability, ionic content of the ore fluids, clay content and mineralization of the material.

To conduct an electrical resistivity test, usually two metal electrodes are used to inject a low-frequency alternating current into the ground and the other two electrodes measure the potential distribution of the subsurface which provides information on the ground. Both current and potential electrodes are usually arranged in linear form or an array during the investigation. Some common array methods include the schlumberger, dipole-dipole, wenner, pole-dipole, and gradient arrays.

Electrical resistivity is one of the most widely used geophysical methods (Jung et al., 2000). The electrical methods were used to delineate seepage zones at two of the four saddle dams of the Som-Kamla-Amba project, Rajasthan State in India (Panthulu et al., 2001). Again the electrical resistivity tomography (ERT), the induced polarization (IP) and Spontaneous potential techniques were used to determine, identify and map probable seepage paths through an earth-fill dam (Wolf Creek dam) in Warren County, Missouri ( Nwokebuihe et al., 2017). Generally, resistivity methods have been deployed in groundwater investigation and environmental engineering to monitor the migration of containment plumes. In civil engineering, the resistivity technique has been used to infer resistive rock formation. In the oil fields, the technique can be used to prospect for conductive ore bodies and for the detection of fractures and cavities in the subsurface.

#### 2.4.1.1 Theory and Basic Principle of Electrical Resistivity

Electrical current is applied to the ground surface and the resultant potential difference measured. Potential difference patterns provide information on the form of subsurface heterogeneities and of their electrical properties.

Consider a cylindrical body of length **L** in meters and uniform cross-sectional area **A** in square meters, having resistance **R** between the end faces. The resistivity is given by;

$$\rho = \frac{RA}{L}$$

(Equation 2. 8)

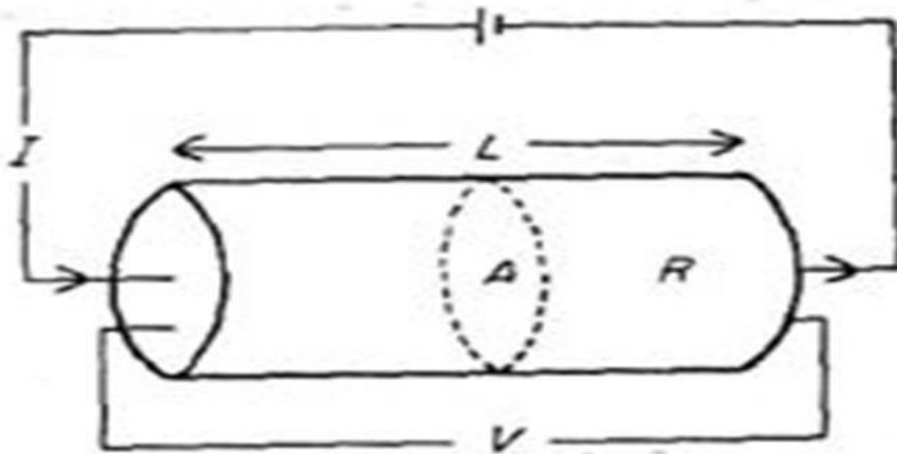


**Figure 2.5 Cylindrical body**

The unit of resistivity  $\rho$  is ohm-meter ( $\Omega\text{m}$ ). Resistance is simply the potential difference recorded across the end surfaces of the cylinder and the resultant current flowing through it,

$$R = \frac{V}{I}$$

where resistance is measured in ohms,  $\Omega$ . Current is measured in amperes(A) and voltage in volts(V).

The simplest theoretical approach to the study of the current flow in the ground surface is to consider the case of a homogeneous isotropic subsurface and a single point current source on the ground surface.

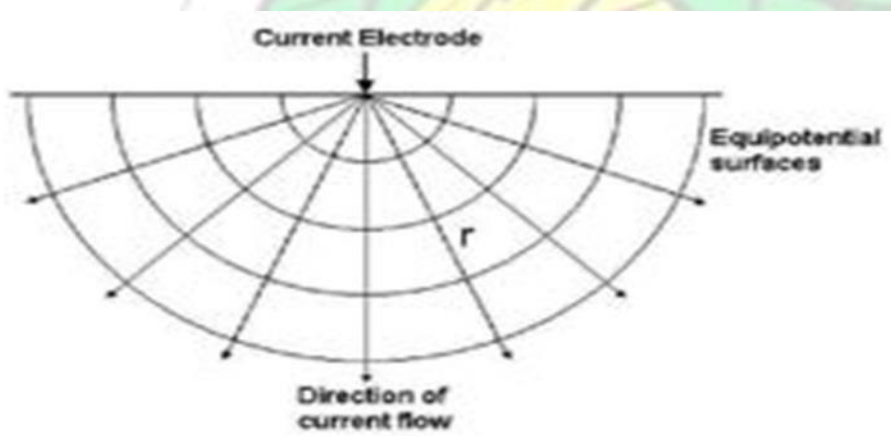


**Figure 2.6 Single point current flow through a homogeneous isotropic subsurface**

The current flows radially from the source of injection. The equipotential surface develops into a hemispherical shape with the current flow perpendicular to the equipotential surface. At some

distance  $r$  from the current point, the hemispherical shell has surface area  $2\pi r^2$ , hence the current density  $J$  is:

$$J = \frac{I}{2\pi r^2} \quad \text{(Equation 2. 9)}$$

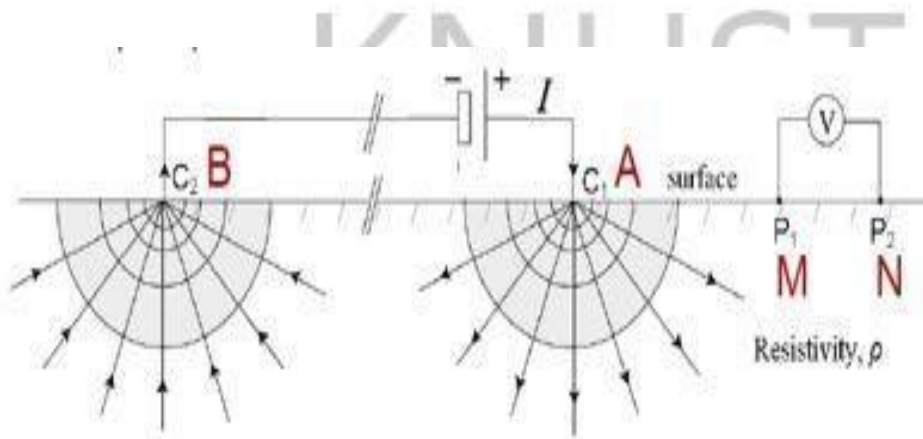


**Figure 2.7 Flow of current from the source and sink through a subsurface**

But in reality, one electrode by itself cannot inject current into half-space. A return electrode is required such that the current flows into the ground via one electrode (source) and exits via another electrode (sink).

The potential difference, therefore, measured at passive electrode  $P_1$  due to current entering and existing at  $C_1$  and  $C_2$  is given by;

$$V_{p1} = \frac{I\rho}{2\pi} \left[ \frac{1}{r_{c1p1}} - \frac{1}{r_{c2p1}} \right] \quad \text{(Equation 2. 10)}$$

The minus sign in the second term of the equation recognizes the change in sign of the current at the source and sink electrodes  $C_1$  and  $C_2$ , and where  $r_{c1p1}$  is the distance between  $P_1$  and  $C_1$  while  $r_{c2p1}$  is the distance between  $P_1$  and  $C_2$ .

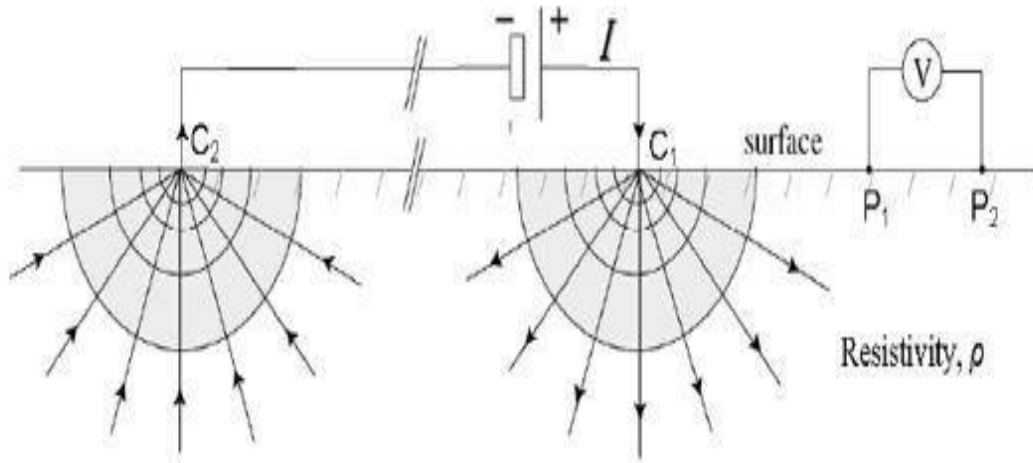


**Figure 2.8 Arrangement of current and potential electrodes**

Again, the potential measured at passive electrode  $P_2$  due to current entering and exiting via active electrodes  $C_1$  and  $C_2$  is;

$$V_{p2} = \frac{I\rho}{2\pi} \left[ \frac{1}{rc_{1p2}} - \frac{1}{rc_{2p2}} \right] \quad \text{(Equation 2.11)}$$

The minus sign in the second term of the equation recognizes the change in sign of the current at the source and sink electrode  $C_1$  and  $C_2$  and where  $rc_{1p2}$  is the distance between  $P_1$  and  $C_1$  while  $rc_{2p2}$  is the distance between  $P_2$  and  $C_2$ .

In practice also, the potential difference between two electrode points is measured rather than an absolute or one potential. Therefore, for a four-electrode array;

$$\Delta V = V_{P1} - V_{P2} \quad \text{(Equation 2.12)}$$

$$\Delta V = \frac{I\rho}{2\pi} \left[ \frac{1}{rc_{1p1}} - \frac{1}{rc_{2p1}} - \frac{1}{rc_{1p2}} + \frac{1}{rc_{2p2}} \right] \quad \text{(Equation 2.13)}$$

calculating for the resistivity  $\rho$  for a half space therefore gives;

$$\frac{\Delta V}{I} \left[ \frac{1}{rc_{1p1}} - \frac{1}{rc_{2p1}} - \frac{1}{rc_{1p2}} + \frac{1}{rc_{2p2}} \right] \rho = \quad \text{(Equation 2.14)}$$

$$\rho = K \quad \text{2.14)}$$

(Equation 2.15)

where  $k$  is a constant called the geometric factor which depends on the type of configuration of both current and potential electrodes.

#### 2.4.1.2 Apparent Resistivity and True Resistivity

Apparent resistivity is the resistivity of a homogeneous half-space which will produce the same response as that measured over the real earth with the same acquisition (Spies, 1986). The apparent resistivity of a geological medium is equal to the resistivity of a fictitious homogeneous and isotropic medium in which, for a given electrode arrangement and current strength, the potential difference measured is equal to that of a given homogeneous medium. The apparent resistivity depends upon the geometry and the resistivity of the element constituting the given medium.

The resistivity obtained for an inhomogeneous subsurface is therefore properly viewed as an apparent resistivity written as:

$$\rho_a = K \frac{\Delta V}{I} \quad \text{(Equation 2.16)}$$

Inversion is the process used to convert the apparent resistivity to the true resistivity of a given subsurface.

#### 2.4.2 Induced Polarization

Induced polarization is used to measure the chargeability of a subsurface. Chargeability is simply defined as how well a material tends to retain electrical charges (Alabi et al., 2010). The technique depends on the electrochemical composition of the subsurface. The induced polarization method is similar to that of electrical resistivity tomography. Both techniques can be applied to a ground surface simultaneously using one equipment.

When electrical current is injected into soil or rock and abruptly interrupted, a difference in potential, which decays with time is observed (Burtman et al., 2015). Decay in Induced Polarization technique is simply the mode of loss of electrical current. This can be fast or slower depending on how mineralized a subsurface is.

Induced polarization has proven to be useful in various environmental and hydrogeological investigations of subsurfaces and has the ability to distinguish between sediments of different lithological composition (Alabi et al., 2010). Induced polarization is also used to map out disseminated sulfides, clay, containment plumes, and groundwater exploration.

Induced polarisation involves measurement of the voltage difference between two potential electrodes. When a mineralized material or metallic mineral block is next to electrolyte-filled pore paths and an electric current flows through the material or rock, an electrochemical overpotential (overvoltage) builds up at the interface between the electron-conducting mineral and the pore solution. The electrochemical forces that oppose current flow are described as polarising the interface and the increase in voltage required to drive current through the interface is called overvoltage.

The IP phenomenon is measured by passing a controlled current through the material and observing the resultant voltage changes with time or with variations of inducing frequency. When the inducing current is put-off, the primary voltage almost drops to secondary response level and then the transient decay voltage diminishes with respect to time. One way of measuring the polarization of the material is by observing the decay phenomenon or the secondary voltage.

In ground that contains no polarisable material, if the current flow is terminated, the voltage between the potential electrodes immediately drops almost to zero.

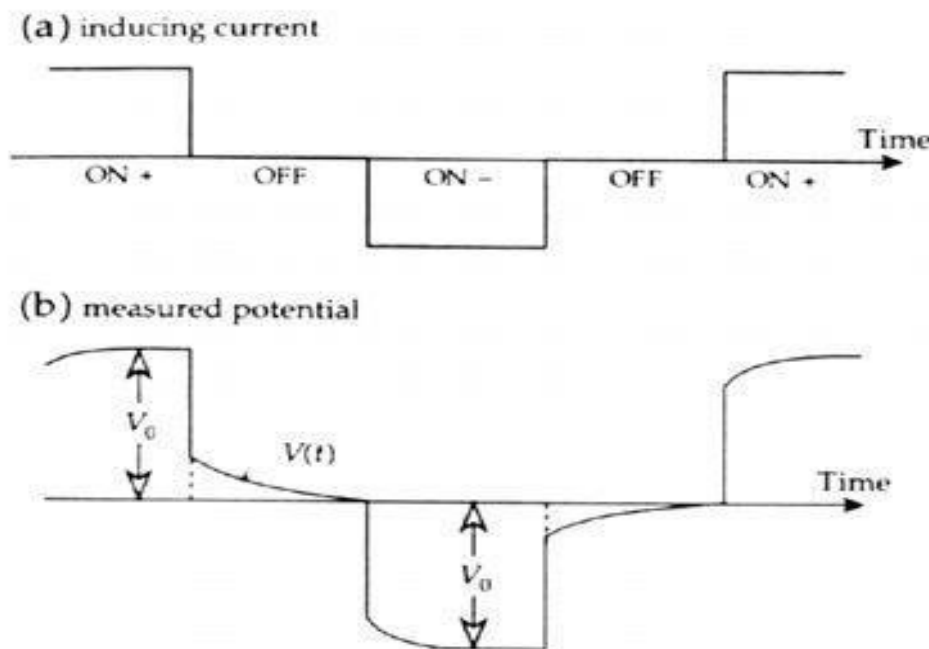


**Figure 2.9 Basic theory for current flow with respect to time**

### 2.4.3 The ABEM Terrameter

The ABEM Terrameter is a state of the art data acquisition system used for measuring resistivity, and time-domain Induced Polarization. The device has a multi-electrode system and a built-in GPS, which automatically locates the instrument position during data acquisition. The instrument which comes with an embedded ARM 9,400MHz Computer system has a 12V, 8Ah internal battery, built-in charger and a 12-18VDC external power giving it the advantage to be used for longer hours.

The ABEM terrameter can be used for both 2D and 3D investigations with electrodes up to 81. A built-in internal electrode selector is used to aid the selection of electrodes during usage. The instrument also comes with an external electrode selector, which uses up to 16384 electrodes depending on the purpose of the survey.

It also has pre-programmed arrays types which include the Schlumberger, Wenner, Dipole-Dipole, Multiple Gradient, Pole-Dipole, and the Pole-Pole arrays

The transmitter has the ability to transmit constant current up to 2500mA maximum and up to  $\pm 600V$  to 1200V peak output voltage. The device also has a self-diagnostics mechanism that can monitor temperature and power dissipation.

The ABEM terrameter LS also has a receiver component which has an input voltage range up to 600V and up to 300Hz flat frequency response.



**Figure 2.10 Geoelectrical imaging system with Terrameter LS**  
(Source: ABEM Instruction Manual)

## 2.5 Application of Geophysical Techniques to Investigate Seepage Conditions in Earth Dams

1. Electrical resistivity and self-potential techniques were deployed to delineate seepage pathways prior to the second phase of grouting of the Crystal Lake Dam located in Washington County, MO (Abdel et al., 2004). Previous measures were carried out to seal the seepage zones by drilling and grouting. However, due to lack of information on the exact seepage paths, the grouting was not effective in the southern toe of the western side of the dam where the bedrock is close to the ground surface. The silty clay dam which is about 10m in depth has its water level lowered from the normal 3.5m to 7m below the crest of the dam due to seepage through the body of the western embankment above a dolomite bedrock.

A total of 9, 2D resistivity profiles were measured using the AGI R-8 Superstring multichannel and multielectrode resistivity unit along the embankment of the dam. Two (2) profiles lines were stationed to the east side of the embankment while seven (7) profiles lines were positioned to the western side (backside of the embankment) of the embankment. Each profile line was 95m in length. The data was processed using the RES2DINV Software to obtain pseudosections. The SP grid was set out after initial results from the resistivity measurement. The results were processed using the Geosoft Oasis Montaj.

From the results processed three resistivity zones were observed along the profiles with different resistivity values and thickness. The first 1 to 2.5m thickness represented the topsoil with moderate resistivity values from 50-150ohm-m; therefore, suggesting low moisture content. A high moisture content ranges from 3.5m to 10m depth representing a silty clay layer with resistivity values 5 ohm-m to 50 ohm-m. The third layer was reported to record resistivity up to 4500ohm-m representing the bedrock. But in some areas within this zone, the moderate resistive layer is recorded suggesting a probability of weathering or fracturing within the zone. Anomalous zones of low resistivity values were also recorded within the highly weathered zones and extend from profile line 5W to 7W suggesting a possible conduit for water flow. Again, SP readings which coincided with the fractured zones within the bedrock recorded high SP readings.

Base on the above findings soil drilling or drilling with grouting was recommended for the anomalous zones mentioned in the resistivity and SP results.

2. A geophysical study was conducted to assess the performance of electrical resistivity tomography (ERT) in the investigation of seepages in the Hsin-Shan Reservoir, which is located on a branch of the keelung River in the Northern part of Taiwan (Lin et al., 2013).

Abnormal seepage appeared on the downstream face of the dam after the dam was reconstructed to raise the water level in the reservoir. A three-number (3nr) 2D electrical resistivity tomography (ERT) was deployed to investigate the abnormal seepage on the dam's left abutment, dam crest, and downstream shell. Line A survey was conducted on the crest. Line B resistivity reading was done on the straight part of the downstream passageway while line C was carried on where the curtain grout was cast during the dam's reconstruction. Also, resistivity measurement was conducted on the downstream shell of line B on a monthly basis for time-lapse measurement to determine the changes in the resistivity of the subsurface. Traverse Line C which passed through the curtain grouting was first examined to determine the effectiveness of the grouting at the left abutment. A low resistivity zone between 20m and 70m was identified at elevation EL80m, which was attributed to the steel pipe for water intake. A vertical band of high resistivity was also recorded from 60m to 100m which was attributed to the solidified grouting which intersected with the traverse line C. For traverse line A, two low resistivity zones were recorded along elevation EL 76m to 84m, since these elevations were above the water level, the low resistivity was attributed to either wetted area or perched underground water due to infiltration of rainwater. Another low resistivity area was found at elevation EL 61m which was also below the abnormal seepage zone. For traverse line B, the low resistive zone was spotted above elevation EL 60m. Two anomalous zones were also recorded at two different locations, stretching from elevation EL 60m to 75m. However, these two low resistivity zones were above the phreatic line of the embankment suggesting two perched areas along the downstream end.

Traverse line B which was the closest to the abnormal seepage zones was used for the timelapse investigation which was conducted on a monthly basis. No apparent anomaly was found by observation of the inverted resistivities recorded for all the investigation for traverse line B. Therefore a more quantitative interpretation using the reservoir level and precipitation was used. A two week accumulated rainfall and reservoir level was used for the interpretation. No significant variation of the reservoir level was recorded within the period. For the low resistive zones, the resistivity areas remain fairly constant irrespective of the variation in precipitation. This then goes on to confirm the presence of perched groundwater. Also, there was a significant correlation between the high resistive areas and precipitation. The resistivity readings at these zones appear to decrease with precipitation which is typical for homogeneous soils.

In conclusion, the two low resistive zones on the traverse line B appear to coincide with the cross-section of that of traverse line A. It was therefore predicted that the seepage pathway

could be through these two zones since they also coincided with the abnormal seepage spots on the dam embankment. It was also concluded from the leakage monitoring data that the amount of abnormal leakage depends largely on precipitation. Results from the 3 ERT 2D pseudo sections on the left abutment, crest, and downstream shell reveal possible underground pathways for anomalous seepage. Results from the time-lapse measurement were used to complement the results from the ERT measurement.



## CHAPTER THREE

### BACKGROUND OF THE KPONG HYDROELECTRIC DAM

#### 3.1 Site Location and Setting of the Kpong Hydroelectric Dams and Dikes

This study was undertaken at the Kpong Hydroelectric Dam located in Akuse in the Eastern Region of Ghana as shown in Figure 3.1. The dam, which is located on the Volta River (Plate 3.1), is about 24km downstream of the Akosombo Dam and 80km away by road from Accra. The main River Dam is 239.74m in length and spans between km 2+635.10 to km 2+874.84. The River Dam is also joined to the west by the West Bulkhead, the Powerhouse, the Centre Bulkhead, the Spillway, and the West Dike all spanning from Km 0+100 to 2+635.10. Also, to the East of the River Dam is the East Dike. The East dike stretches from km 2+875 to 6+460 while the West dike spans from km 0+100 to km 2+176. The West Bulkhead, the Powerhouse, the Centre Bulkhead, and the Spillway spans from Km 2+176 to 2+635. The maximum designed elevation of the crest of the river dam and the two dikes are 18.25 National Datum level (NDL). The dikes are provided with both total and partial core trench cutoffs on the east and west banks. The functions of the cutoff trenches are to reduce the loss of reservoir water through the foundation or to prevent the subsurface erosion by piping through the foundation.

While the total cut-off trench for the west dike is established between km 2+038 to km 2+176 that of the East Dike starts from km 2+875 and ends at km 3 + 060. Also, the partial cut-off trenches for both West and East Dikes span from km 0+100 to km 2+038 and km 3+060 to 6+460 respectively. Some differences exist between the excavation for both total and partial cut-off trenches. While the total core cutoff trench is excavated to the bedrock, the partial core cutoff trench is excavated to only 3m deep into the overburden foundation. The excavation is also dependent on the competence of the overburden foundation. A weaker overburden, therefore, results in a total cut-off trench and vice versa.

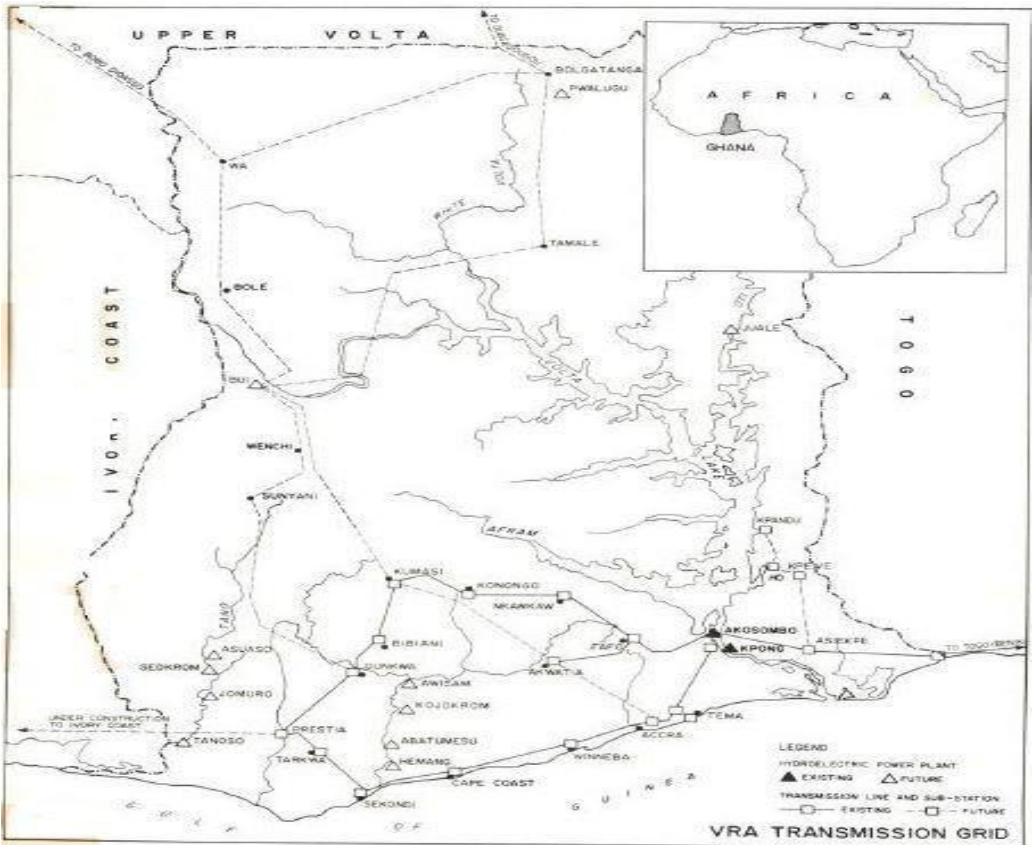


**Figure 3.1 Location of Kpong Hydroelectric Dam with respect to Ghana**  
 (Source: Geotechnical completion report of the Kpong Hydroelectric Dam)

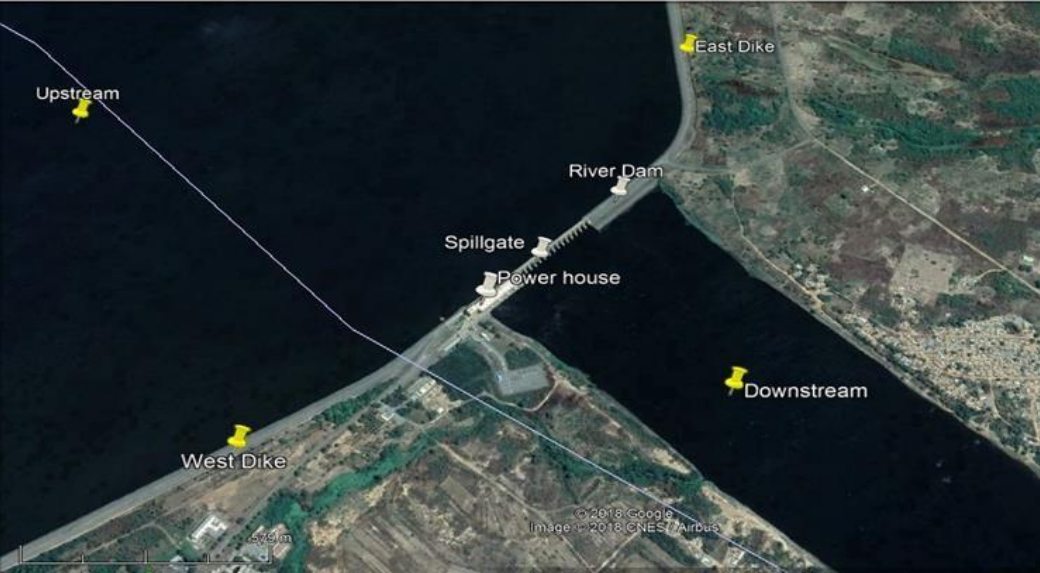


**Figure 3.2 Kpong Hydroelectric Dam**  
 (Source: Google image)

### **3.2 Bedrock of Kpong Hydroelectric Dam**

The bedrock at the dam location consists essentially of garnetiferous hornblende gneiss belonging to the Precambrian Dahomean series. Local intrusions of the pyroxenite occur in the rock foundation of the East Dike from km 4+184 to km 4+320.

The gneiss consists of dark or dark green hornblende, oligoclase quartz, and red garnets. It is massive, strong, medium to coarse-grained, light to dark grey in colour and also foliated. The bedrock on both banks of the river is covered with river alluvium to a ground elevation of about 12m. However, at a higher elevation, residual soils derived from weathering of the in situ rock overlies the bedrock.

Three joint sets occur in the gneiss, the major one which is parallel to the foliation strikes northeast to southwest and dipping  $15^{\circ}$  to  $25^{\circ}$  south-easterly. The other two being subvertical sets striking at  $85^{\circ}$  and  $175^{\circ}$ . Spacing varies in general from an average of about 50cm for foliation joints and from 30cm to several meters for the other two subvertical joint sets. Shear zones, usually less than 50cm thick occur, locally within the gneiss generally conformably to the foliation planes. A fourth set of subvertical joints occur within the total cut-off area of the East Dike. It strikes at  $50^{\circ}$ .

Pyroxenite intrusions of the Gneiss bedrock outcrop in zones several meters thick between km 4+100 and 4+320. The rock in this zone is about 18m higher than the rock surface within the river channel and also exhibits deep weathering and is highly jointed and sheared.

The rock quality for the garnetiferous hornblende gneiss is mostly excellent with RQD's above 90% with actual core recovery close to 100% within the location of the Kpong Dam. Where pyroxenite intrusions occur, the RQD is about 40% with core recoveries between 90 and 100%. The coefficient of rock mass permeability is in the range of  $1 \times 10^{-4}$  to  $1 \times 10^5$  cm/s. The depth of weathering in the rock at the rock/overburden interface varies from a few centimeters to 16m but is generally less than 1.5m. The bedrock is exposed only in the riverbed. The pyroxenite intrusive rock is normally highly sheared and is exposed on the East Dike axis, and strikes at  $60^{\circ}$  with a dip of  $15^{\circ}$ .

### **3.3 Overburden Material of East Dike**

The east dike is built on an overburden material. The elevation of the overburden at the east Dike varies from 12m National Datum Level to 2m National Datum Level at the end of the dike at km 6+460. The overburden is mainly made up of two layers of alluvial deposits.

These consist of a lower layer of a more permeable deposit of medium dense to dense sand and gravels overlaid by more fine-grained firms to stiff silts and clays.

The lower granular strata consist of layers of slightly cemented coarse sand and gravel 3m in thickness in areas directly overlying the bedrock, followed by sand and silty sand at higher levels. The upper fine-grained soils consist of relatively more impervious silts and clays. The study section is, however, made up of sand and gravel overlain by a silt and clay material up to an average elevation of 12m National Datum Level.

### **3.4 Composition of the Kpong East Dike**

The following were deduced from the Geotechnical Completion Report (Acres International Limited, 1981) of the Kpong Hydroelectric Project:

The east dike is a typical zoned embankment made up of mainly three sections namely; the Core, the Filter and Fill Materials. The core which is composed of impervious fill consists essentially of silty clay, the clay fraction varying between 25% and 65%. Also, the designed plasticity index of the impervious core is between 10% and 40%.

The filter material is placed above the impervious layer. The filter layer is made up of sand mixed with about 10% crushed fines. The major function of the filter is to prevent the washout of materials from the impervious layer. Again, it serves as a drain for seepage water from the reservoir.

At both the upstream and downstream of the dike is the fine rockfill of varying sizes from 150mm to 0.074mm crush rock. Lastly, coarse rock fill, up to 750mm, is laid at the upstream side of the dike. Both the fine and coarse rock fill collectively is termed the fill. Its purpose is to receive the load from the water and transfer it safely to the ground.

Also, relief wells sunk to the bedrock have also been installed along the first berm of the East Dike at varying intervals and at locations depending on the permeability and thickness of strata of the bedrock. These wells were designed with slotted and unslotted sections PVC pipes.

The section of the east dike studied lies between Km 4+705 to 4+945 and falls within the partial cutoff trench of the East Dike. A typical section of the partial cutoff trench is shown in Figure 3.3.

Also for the section under study, the overburden material has an average elevation of 12m NDL with reference from the river bed at elevation 0.00m NDL as shown in Figure 3.4.

However, the overburden comes into contact with the bedrock outcropping at elevation 4m NDL at the riverbank of the east dike in the study section. This gives the thickness of the overburden to be approximately 8m. Therefore, a 6m thick layer of the overburden is made up of sand and gravel and is overlain by silt and clay of varying proportion of 2m depth. Also, the maximum elevation measured on the crest of the dike is 18m NDL. The overall structural height of the Dike can, therefore, be estimated to be 6m thick from the overburden.

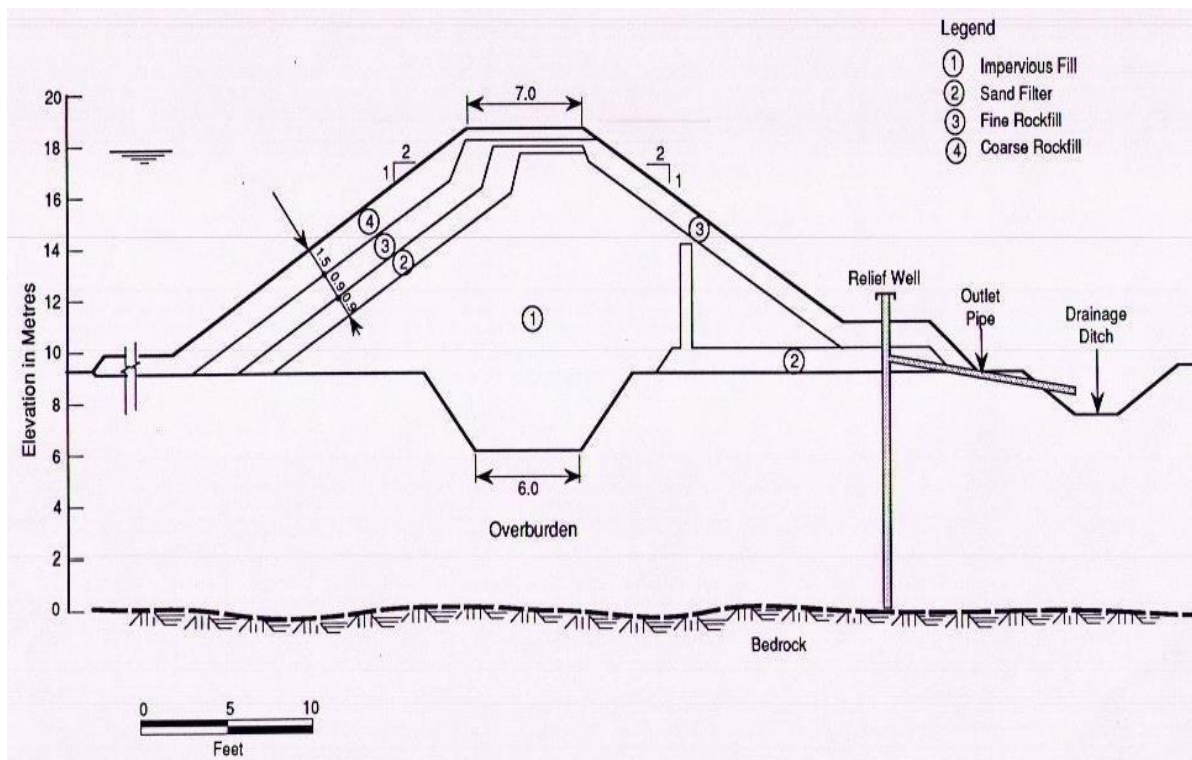


**Figure 3.3 Typical partial cut-off section of the East Dike**  
**(Source: Geotechnical completion report of the Kpong Hydroelectric Dam)**

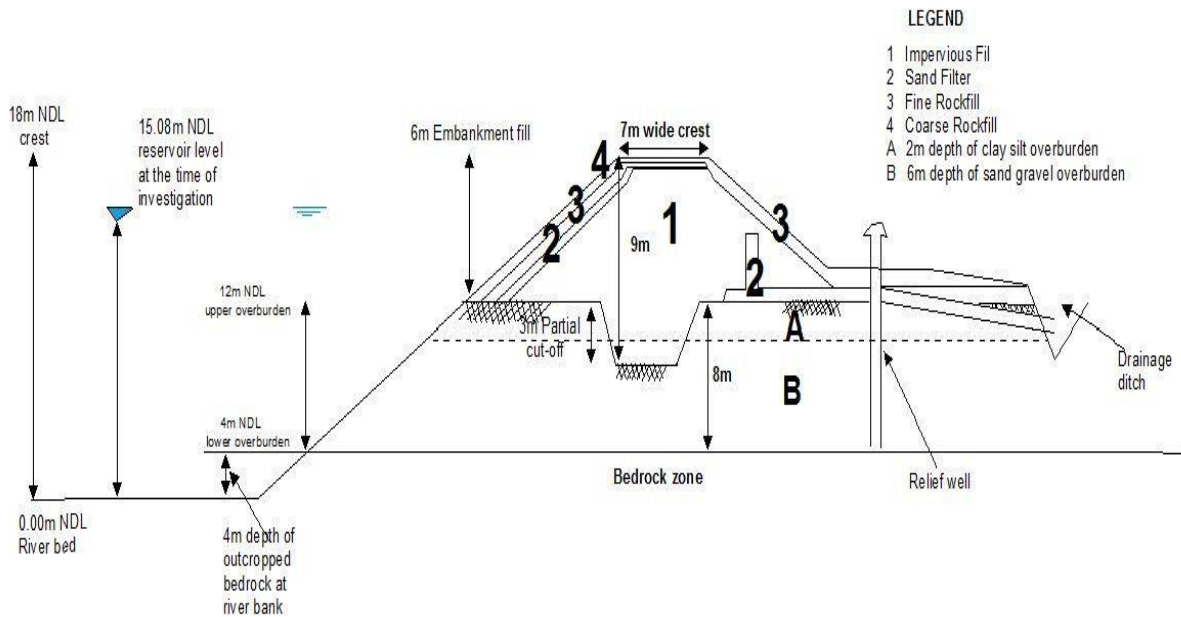


**Figure 3.4 Detail representation of dike in the study section.**

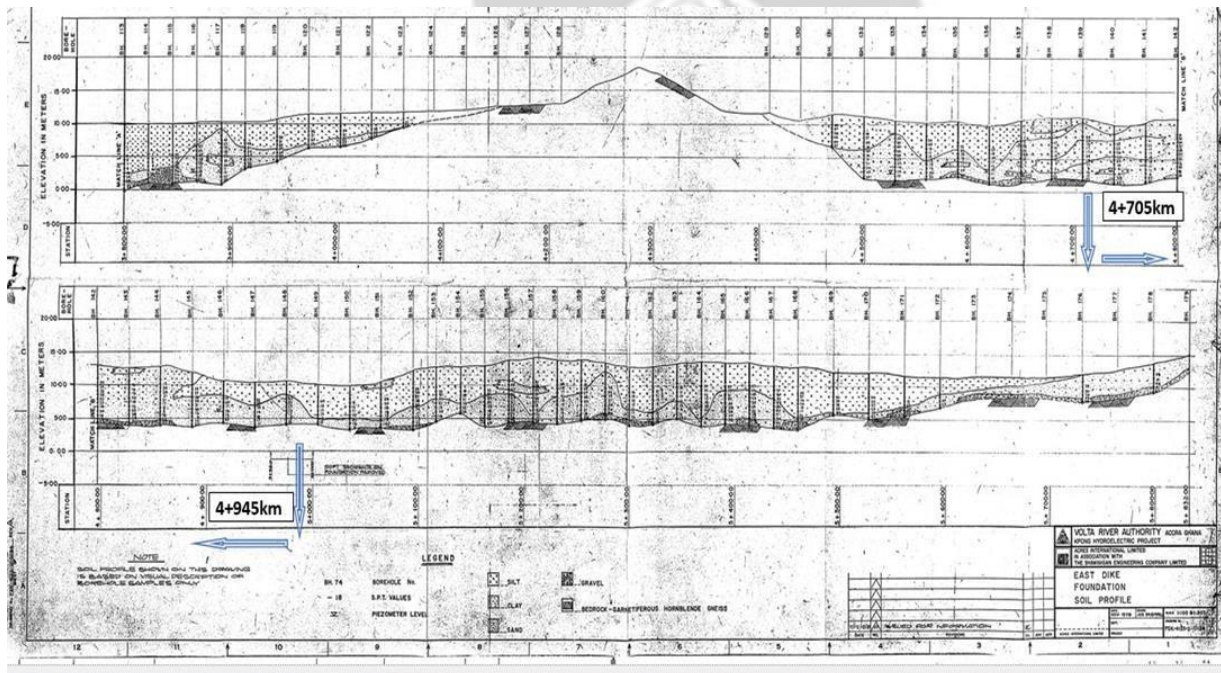


**Figure 3.5 Overburden stratigraphy of the East Dike showing study section (Source: Geotechnical completion report of the Kpong Hydroelectric Dam)**

### 3.5 Location of Unplanned Seepage Points

The Kpong Hydroelectric Dam has recorded a total of three unplanned seepage locations on both West and East Dikes as of December 2018. However, the location of the unplanned seepage point at the section of the dam being studied is around km 4+802 and on the

downstream side of the East Dike with coordinates 6°8'28.00"N latitude and 0° 7'39.98"E longitude. Plate 3.2 shows the unplanned seepage point.



**Plate 3. 1 Unplanned seepage location (6°8'28.00"N latitude and 0° 7'39.98"E longitude)**

## CHAPTER FOUR

### METHODOLOGY

#### 4.1 Survey Plan

The investigation was conducted on four (4) traverse lines set out on the East Dike and include T1, T2, T3, and T4. Each traverse line was about 240m in length and stationed between Km 4+705 to 4+945 on the East dike. Detail information on the traverses is provided in Table 4.1. A google image showing the orientation of the traverse lines and the unplanned seepage point is provided in Figure 4.1.

**Table 4.1 Coordinate of survey locations**

TRAVERSE LINE	LOCATION	DISTANCE FROM T1 /m	START POINT		END POINT	
			Coordinates	Elevation /m NDL	Coordinates	Elevation /m NDL

T1	CREST	0	N06°08'24. 7''	18	N06°08'32. 4''	18
			E000°07'38 .6''		E000°07'38. 0''	
T2	SLOPY SIDE	12	N06°08'24. 7''	16	N06°08'32. 4''	16
			E000°07'39. 2'		E000°07'38 .3''	
T3	1st BERM	30	N06°08'24. 8''	12	N06°08'32. 5''	12
			E000°07'39. 5''		E000°07'38. 8''	
T4	1.5m TO UNCONTROL LED SEEPAGE POINT	48	N06°08'24. 8''	12	N06°08'31. 7''	12
			E000°07'40. 3''		E000°07'39. 5''	



Figure 4.1 Orientation of traverse lines

## 4.2 Resistivity and Induced Polarization Measurement

The data for both resistivity and induced polarization were acquired simultaneously along the four (4) traverse lines using the ABEM Terrameter LS.

The gradient plus array type (Figure 4.2) was adopted for the investigation with a 2m electrode spacing and a 4x21 cable layout. A total of 240m length of traverse line was covered for each of the four traverse lines. The targeted depth of investigation considered was 25m deep.

The setting up process was done using the standard cable configuration of the ABEM Terrameter LS. It comprises four cables of length 100m each with 21 electrodes take-out on each cable. The first and last reel of each cable was overlapped to attain a full layout of 81 electrodes. A “roll along” method was also adopted for the survey of each 240m traverse line. The 3 cable first, 1 cable forward was adopted for the roll-along in order to cover the entire 240m traverse line.



Figure 4. 2 Multiple gradient array

(Source ABEM)



Plate 4.1 Measurement of resistivity and induced polarization in progress

### **4.3 Data Processing**

The data was downloaded and stored on a laptop computer for processing.

RES2VIN software was used for processing the data. ArcGIS was also used to make sketches and delineate seepage zones and possible seepage pathways on the pseudo sections obtained.

## **CHAPTER FIVE**

### **RESULTS AND DISCUSSION**

#### **5.1 Results of Electrical Resistivity Tomography of the Study Section of the East Dike**

A total of four (4) traverse lines were established at intervals along the embankment starting from the top of the crest to the toe drain.

Traverse line 1 was established on top of the 7m wide embankment crest. The average elevation of the crest measured is 18m National Datum Level (NDL). The thickness of the east dike is averagely 6m from the crest to the top of the overburden soil at the study section. The inverted resistivity cross-section of traverse line 1 in Figure 4.4 shows a high resistive layer between 700 $\Omega$ m to 2000 $\Omega$ m within the first 5m depth of investigation. This layer might be made up of the coarse and fine rockfill and possibly dry sand filter.

Between the 5m to a 14m depth of investigation are layers of varying resistivity ranging from as low as 10 $\Omega$ m to 800 $\Omega$ m high resistivity. This depth is inferred to span from 5m below the crest of the dike to the overburden-bedrock interface. Materials within this depth are therefore predicted to be composed of a portion of the silty clay core, an upper silt and clay overburden material underlain by sand and gravel overburden material.

However, particular interest should be paid to distances 42m to 78m, 96m to 112m, 122m to 138m, 170m to 180m and 232m to 270m within the overburden between the depth of 9m and 11m. These zones exhibited very low resistivity from 10 $\Omega$ m to 50 $\Omega$ m within the lower layer of the sand gravel overburden material, and might, therefore, be possible seepage zones.

These inferred seepage zones are also bounded by a 100  $\Omega$ m to 170  $\Omega$ m medium resistivity layers and might be moist zones within the overburden layer. Again, from distance 164m to

192m is a zone with medium resistivity from 100  $\Omega\text{m}$  to 170  $\Omega\text{m}$  spanning downwards from the overburden to the bedrock. This zone might be caused by a possible fractured bedrock.

Underlying the 14m depth of investigation is another layer with resistivity ranging from a 180 $\Omega\text{m}$  to about 3500 $\Omega\text{m}$  high resistivity depicting a bedrock. The 180 $\Omega\text{m}$  resistivity recorded is inferred to be within the interface of the overburden and the bedrock and might be moist sand and gravel overburden.

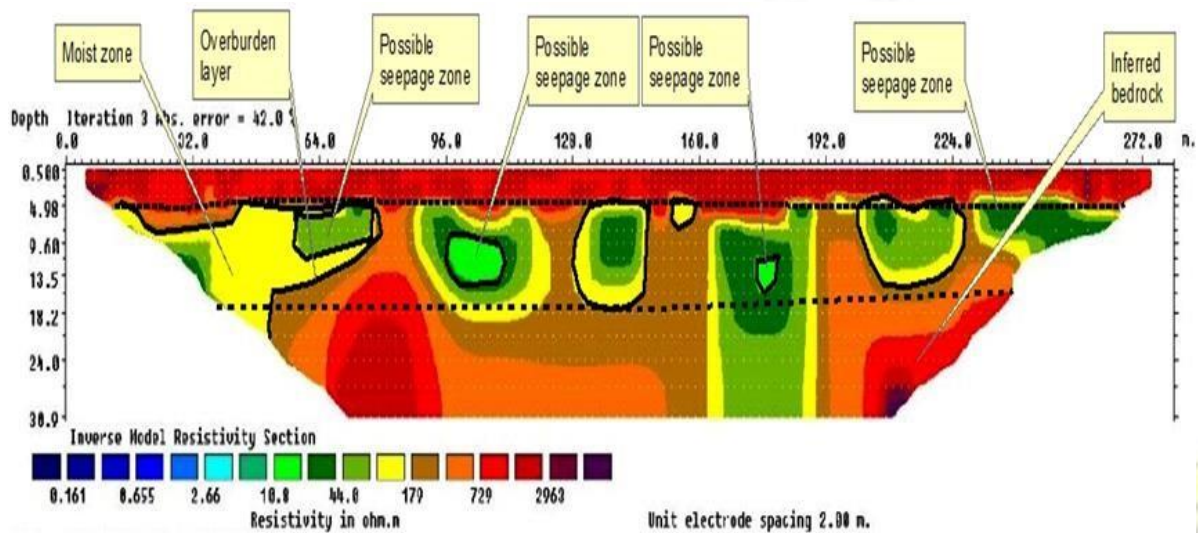


**Figure 5.1 Traverse Line 1 Resistivity Pseudosection**

Traverse line 2 which was established along the slope of the dike and at an elevation of 16m NDL. It also measures a distance of 13m from traverse line 1. The top layer shows a medium resistivity from 65 $\Omega\text{m}$  to 700 $\Omega\text{m}$  along the whole stretch of the investigation. This layer which is about 1m deep is inferred to be the fine rock fill layer of the dike.

Underlying the 1m depth fine rock fill layer to a depth of about 4m is a very low resistivity material ( $<4\Omega\text{m}$ ). It is inferred that this depth spans through the vertical sand filter of the dike. Therefore, the very low resistivity ( $<4\Omega\text{m}$ ) recorded would be as a result of the sand filter layer being saturated with seepage water. Also, extending from the 4m depth to about 9m depth are pockets of low resistivity zones also with low resistivity  $<4\Omega\text{m}$  occurring within the silt clay and sand gravel overburden material. These zones might be potential seepage zones and include distances 10m to 26m, 50m to 62m and 90m to 96m. Also, from the 9m depth to about 12m depth is a zone with resistivity from 300 $\Omega\text{m}$  to about 1000 $\Omega\text{m}$ , and might be zones of consolidation within the sand gravel overburden. Beyond the 12m depth is a very high resistivity ( $>1500\Omega\text{m}$ ) zone and may be an indication of the underlying competent bedrock.

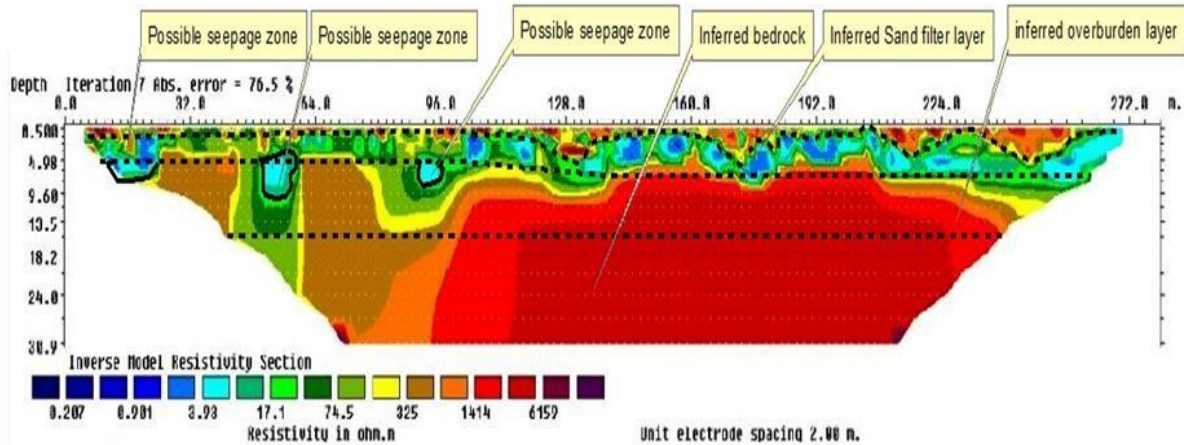


**Figure 5.2 Traverse Line 2 Resistivity Pseudosection**

Traverse line 3 was stationed along the first berm of the east dike and directly in front of eight (8) relief wells (RW) in the order of RW 153, RW 154, RW155, RW156, RW157, RW158, RW 160 and RW161 from the beginning of the traverse line 3 and at varying intervals as shown in Figure 5.4. Table 5. 1 further shows the various measured distances with respect to the start of traverse line 3 for the various relief wells.

Traverse line 3 was stationed at a distance of 18m away from traverse line 2 and at an average elevation of 12m NDL. Seepage water levels measured in the relief wells (7 relief wells) at the study section is shown in Figure 5.5. The readings suggest that relief wells RW153, RW154, RW155, and RW156 were not discharging at their optimum level for the 2018 review year. This may be due to possible siltation especially in the horizontal portion of the relief wells. A relief well is considered to be discharging at its optimum level if the measured water level in the vertical portion of the relief well is below or at the same level as the invert level of the drain pipe or horizontal portion of the relief well (Figure 5.6) . A possible silted relief well has measured seepage water level above the invert level of the horizontal pipe or drain pipe.

The resistivity image obtained for traverse line 3 showed a thin layer of about 1-meter depth having a resistivity up to about 500Ωm. This depth is predicted to be the fine rockfill depth around the relief wells.

Beneath this 1m thin layer to a depth of about 6m, is a low resistivity material (< 25Ωm) from 102m to 270m distance. This layer is inferred to occur within the silt-clay underlain by sand gravel overburden layer. It is anticipated that the flow of seepage water migrating from the reservoir through the overburden would find its way into the relief wells, where it would be

subsequently drained out. Therefore, the low resistivity (<25Ωm) at this depth could be as a result of the concentration of seepage water within the sand gravel overburden from the reservoir.

Again, a low resistivity channel of <25Ωm is recorded from distance 78m to 96m and at a depth ranging from 4.5m to 28m. This low resistivity channel recorded could be caused by either a fractured bedrock or a build-up of seepage water around a possible silted relief well. A fractured bedrock could admit seepage water into its space, thus creating such a low resistivity channel. Also, as shown in Table 5.1, relief well RW 156 has close proximity (107m) to this low resistivity channel. This relief well is highly silted (1.28m water level above the invert level of the drain pipe) compared to other relief wells in Figure 5.5. Seepage water might have built around this relief well, thus, creating such a low resistivity channel. Therefore, possible seepage zones include distances 44m to 78m and 82m to 96m which recorded low resistivity of <25Ωm within the overburden layer.

Below the 6m level is a depth with varying resistivity from >500Ωm. This layer is inferred to be a competent layer such as the bedrock.

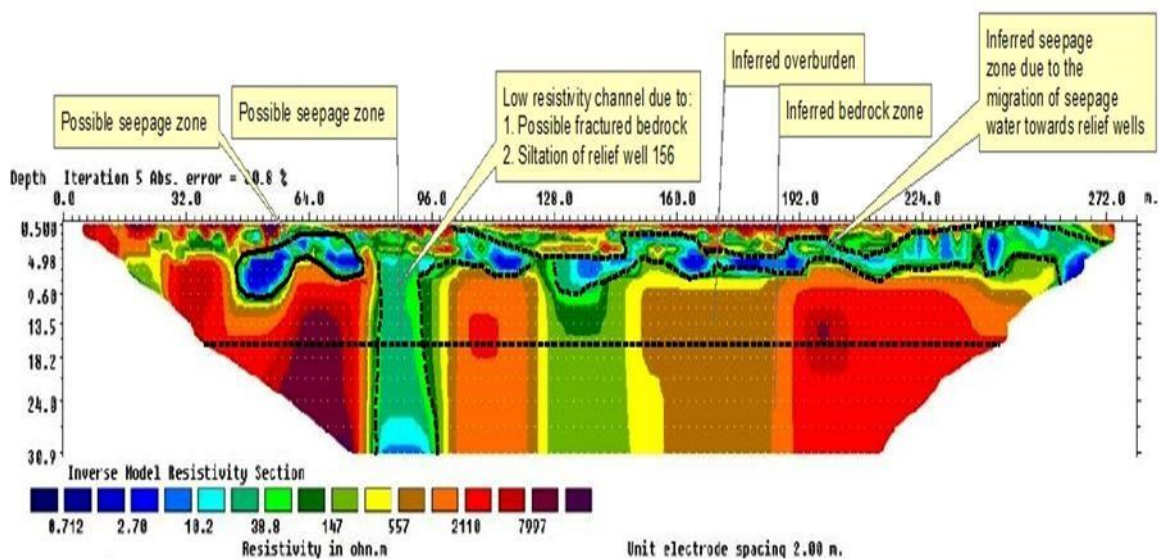


**Figure 5.3 Traverse Line 3 Resistivity Pseudosection**



Figure 5.4 Google view of Relief Wells positions

Table 5.1 Respective distance of Relief Wells

Relief Well	Distance(m) with respect to the start of traverse line 3
RW153	25
RW154	49
RW155	79
RW156	107
RW157	140
RW158	173
RW160	197
RW161	232

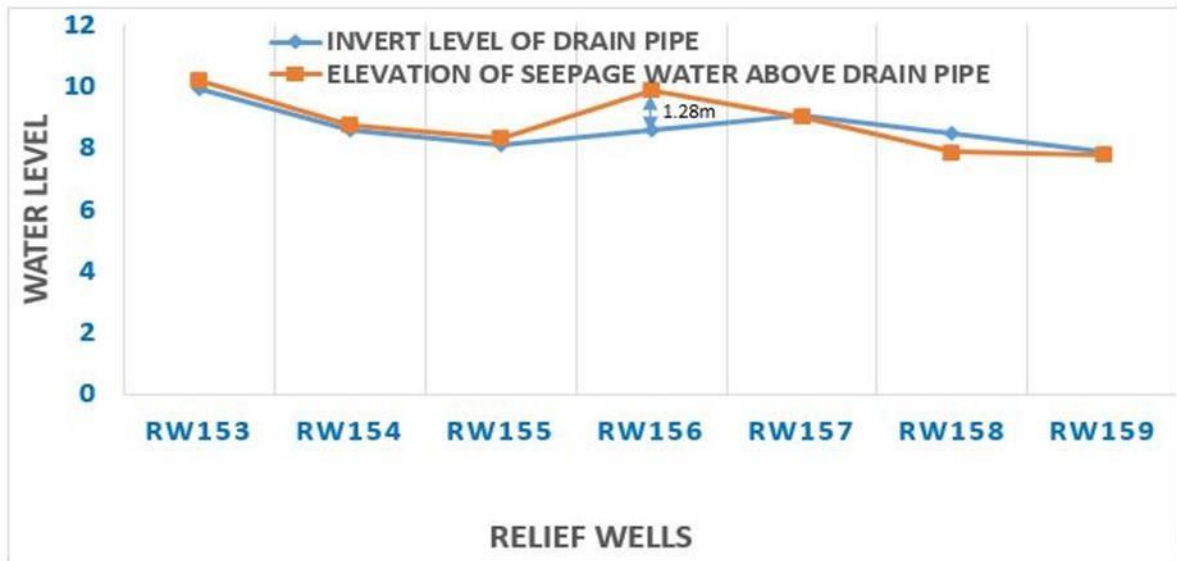


Figure 5.5 Graph of relief wells against measured seepage water level for 2018

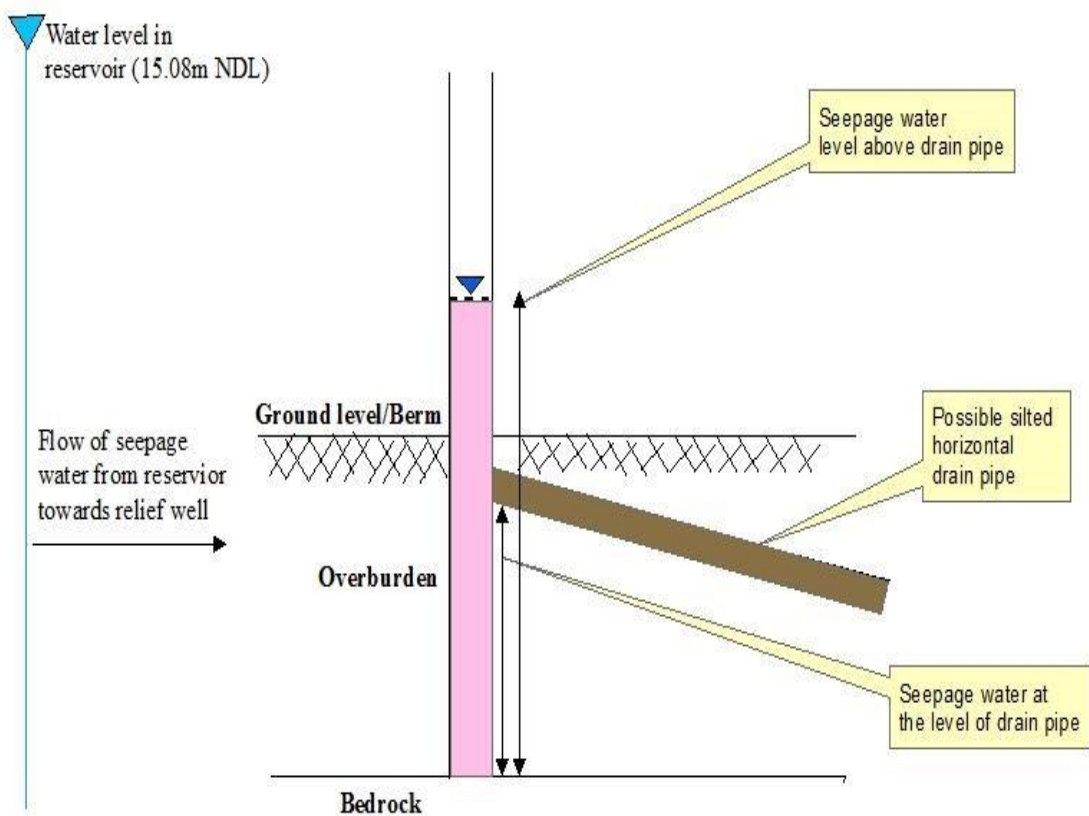


Figure 5.6 Possible siltation of relief well

The traverse line 4 was established at a distance of 18m away from traverse line 3 and 1.5m distance before the unplanned seepage point. This unplanned seepage point on the ground also measures a distance of 98m with respect to the start of traverse line 4.

This survey line was conducted on the overburden material of the east dike on the maximum elevation of 12m NDL.

The pseudo section of traverse line 4 exhibit resistivity between  $10\Omega\text{m}$  to  $50\Omega\text{m}$  within an average 3m depth of investigation. Beneath the 3m depth to about 8m depth is another zone with a resistivity of about  $70\Omega\text{m}$ - $150\Omega\text{m}$ . These two depth ranges which could be saturated, are inferred to occur within the overburden materials, namely; silt and clay underlain by sand and gravel material respectively. Below the 8m depth are zones of high resistivity  $>400\Omega\text{m}$ , which could be a competent layer.

However, particular attention must be paid to zones between distances 50m to 58m and 90m to 98m. These distances could be potential seepage zones with corresponding very low resistivity of about  $2\Omega\text{m}$  and at a depth between 5m and 9m.

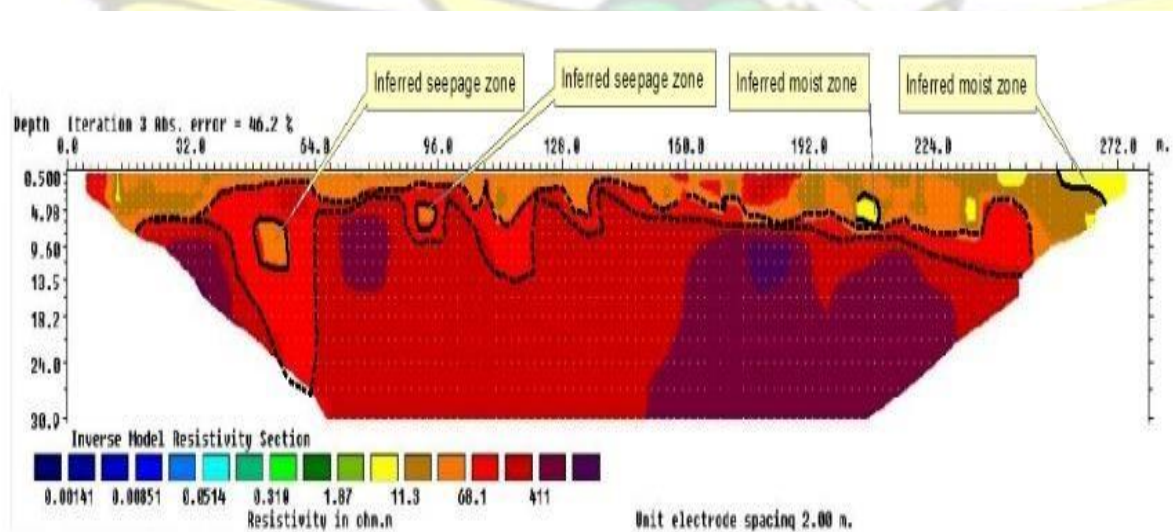


**Figure 5.7 Traverse Line 4 Resistivity Pseudosection**

## 5.2 Results of Induced Polarization (IP) Survey of the Study Section of the East Dike

Induced polarization (IP) data were picked and processed simultaneously with the Electrical Resistivity Tomography (ERT) data.

There are three main different zones inferred in traverse line 1. The first 5m depth of investigation indicates a very low chargeability of 10msec to 300msec while the 5m to 14m

depth exhibited pockets of high chargeability of 600msec to 900msec perhaps due to the presence of the silt clay overburden. Below the 14m depth of investigation also indicates a very low chargeability of 10msec to 300msec, perhaps depicting the bedrock zone.

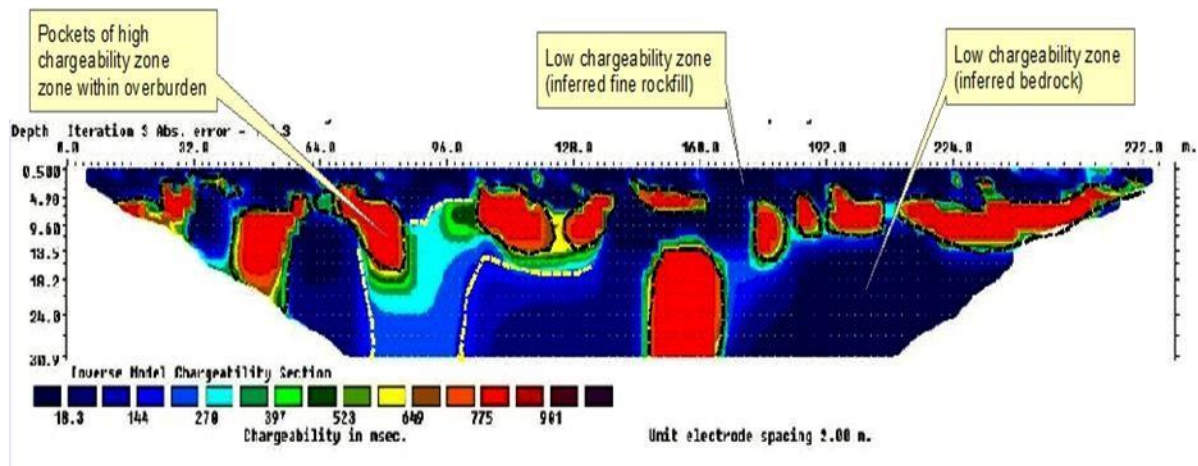


**Figure 5.8 Traverse Line 1 Induced Polarization Pseudosection**

For traverse line 2, varying chargeability from 12msec low to about 90msec high is recorded at a maximum depth of about 6m depth of investigation. This depth is inferred to span from the fine rockfill zone, the sand filter zone, and the upper silt and clay overburden material.

Underneath the 6m depth are other zones of low chargeability <1msec which might be a consolidated portion of the sand and gravel overburden material underlain by a competent bedrock.

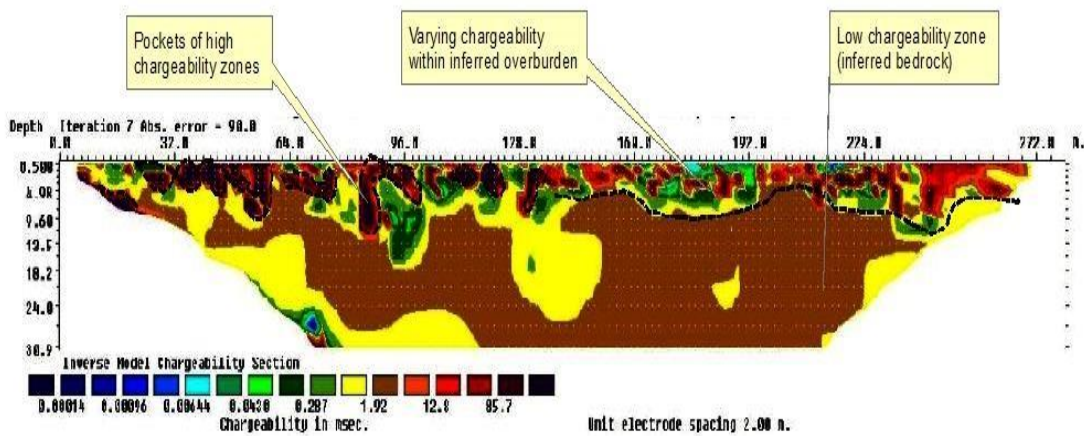


**Figure 5.9 Traverse Line 2 Induced Polarization Pseudosection**

For traverse line 3, a thin layer of 0.04msec to 0.4msec very low chargeability is predicted up to a 2m depth of investigation. This layer is inferred to be the fine rock fill layer of the dike. From a 2m depth to an average of 6m is a zone inferred to have chargeability >50msec and might be a moist sand and gravel overburden. Below the 6m depth is a zone with chargeability <5msec and is predicted to fall within the bedrock zone.

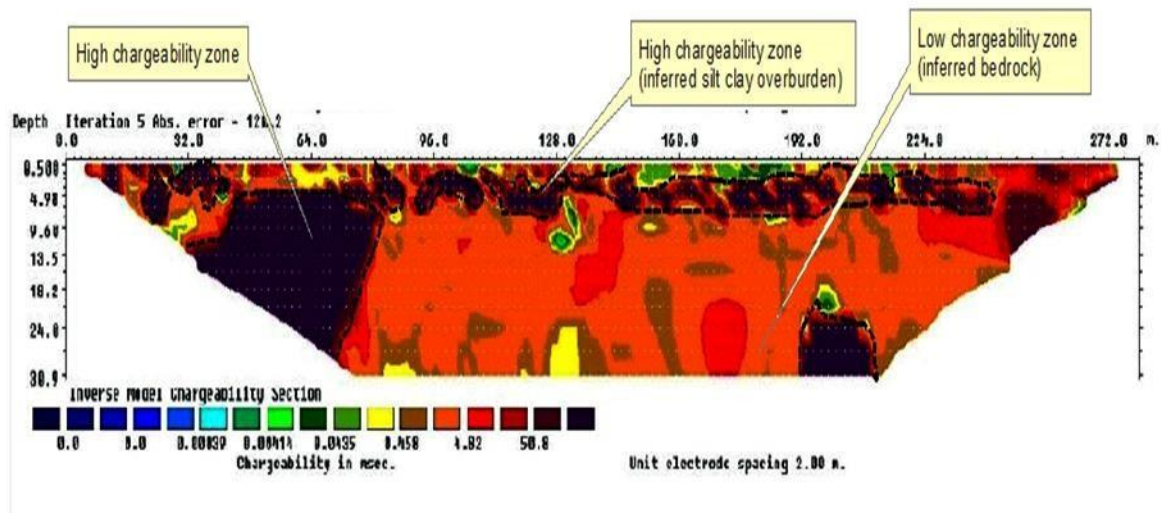


**Figure 5.10 Traverse Line 3 Induced Polarization Pseudosection**

Traverse line 4 was conducted over the overburden material made up of upper silt and clay underlain by sand and gravel. The entire depth of investigation appears to be saturated with an average low chargeability of <300msec, with pockets of zones, also recording chargeability from 350msec to 400msec and includes distances; 64m -78m, 160m- 164m and 182m -186m. From the analysis of results obtained by the induced polarization technique, the results from the four (4) sections do not clearly show the seepage zones and thus, difficult to delineate the potential pathway using the results from the induced polarization.

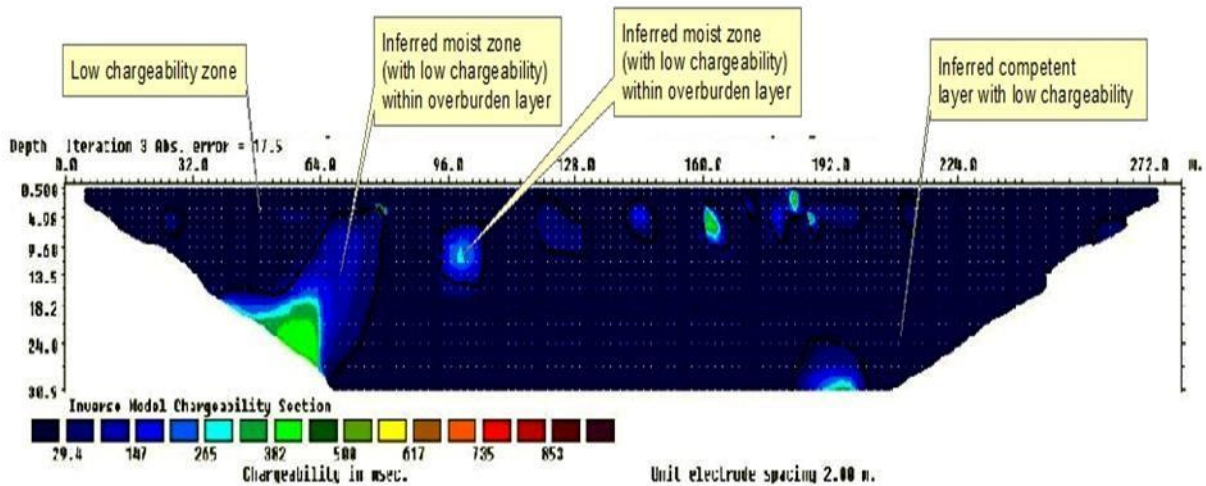


**Figure 5.11 Traverse Line 4 Induced Polarization Pseudosection**

### 5.3 Delineation of potential seepage pathway

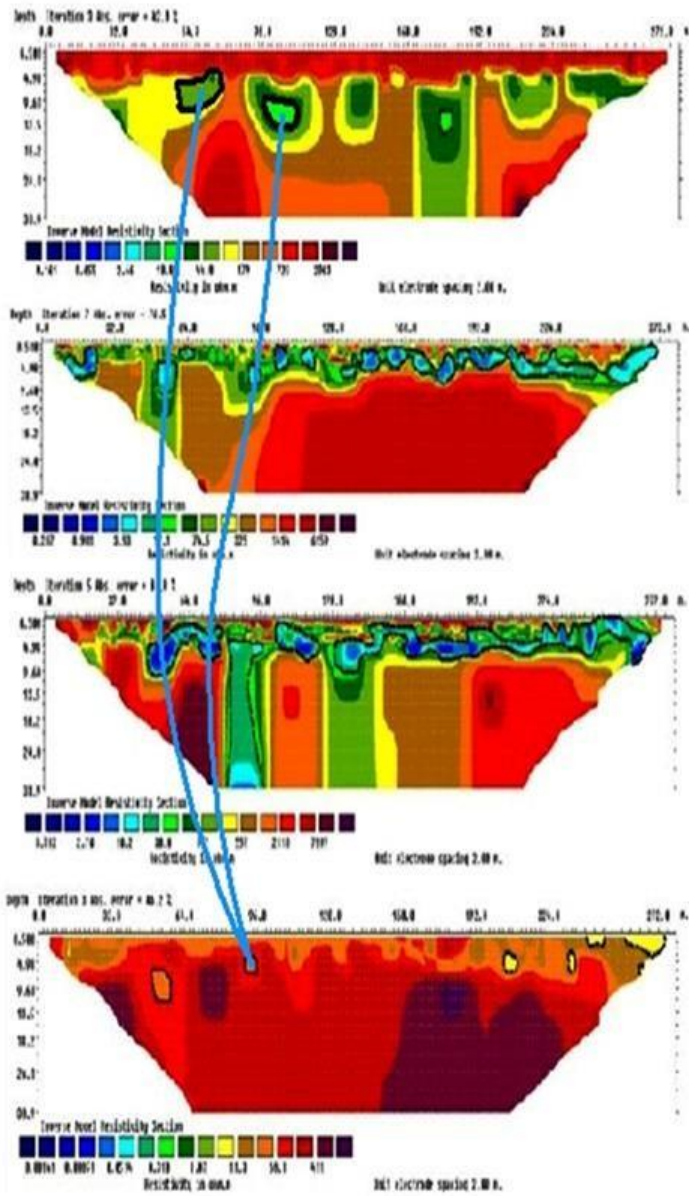
Based on the results of the resistivity sections, the potential unplanned seepage pathway can be said to have been developed within the lower sand and gravel layer of the overburden material.

The potential unplanned seepage pathway can be delineated as follows:

Between distances 42m to 78m and 96m to 112m occurring at an average depth of 11m for traverse line 1. For traverse line 2, an unplanned seepage pathway might occur between distances 50m to 62m and 90m to 96m at 9m average depth of the lower sand gravel overburden material. Also, for traverse line 3, a potential unplanned seepage pathway is predicted to occur between distances 44m to 78m, within the sand and gravel overburden at an average depth of 5m. Finally, importance should be attached to the zone between distances 90m to 98m at a depth of 5m for traverse line 4. This zone could be a potential pathway for the unplanned seepage water due to its close proximity to an unplanned seepage point identified at the downstream of the east dike.

Below is a schematic representation of the possible delineated unplanned seepage pathway from the resistivity results.

**a. Possible delineated unplanned seepage pathway from resistivity results combined**



**Legend**  
 Possible delineated seepage pathway

b. Sectional view of the delineated unplanned seepage pathway from resistivity results



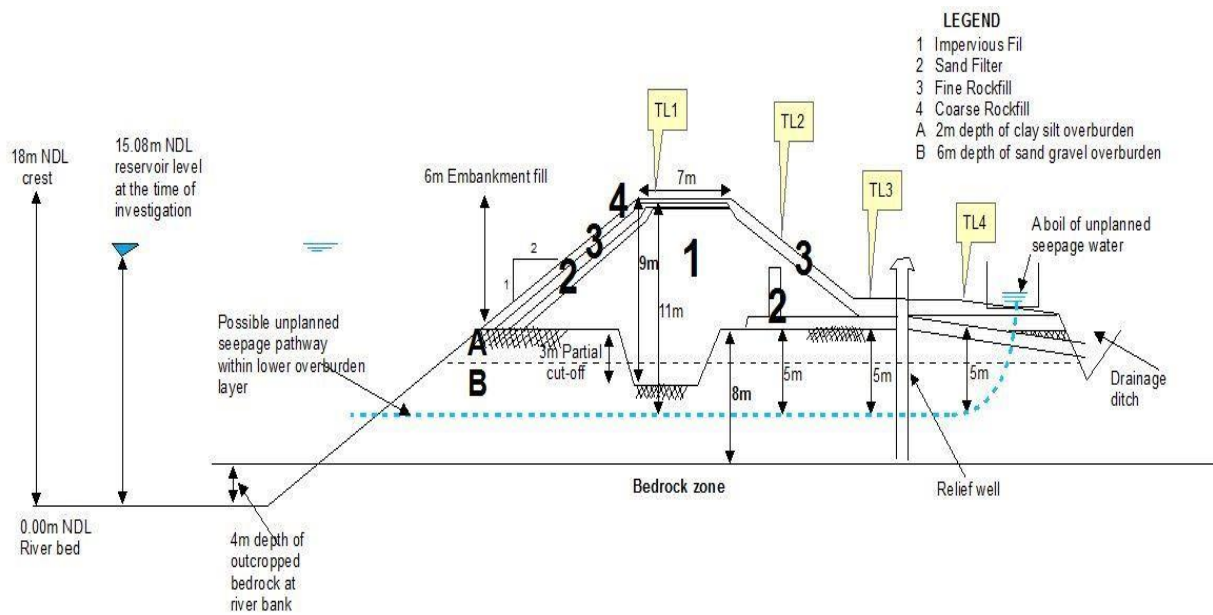


**Figure 5.12 (a) Possible delineated unplanned seepage pathway from resistivity results combined (b) A sectional view of the delineated unplanned seepage pathway from resistivity results**

## CHAPTER SIX

### CONCLUSION AND RECOMMENDATION

#### 6.1 Conclusion

This research was conducted to explore the possibility of using the electrical resistivity tomography and the induced polarization in detecting unplanned seepage condition on the east dike of the Kpong Hydroelectric dam and delineating possible seepage pathway or channel. Based on the results and analysis made with the help of geotechnical design information of the East Dike, the following conclusions were drawn.

- That the electrical resistivity method is able to detect seepage zones and delineate possible unplanned seepage pathways. The unplanned seepage pathway is predicted to be within the lower sand and gravel overburden material
- That the potential seepage zones inferred is at an average elevation of 7m NDAL and includes 42m to 78m, 96m to 112m, 122m to 138m 170m to 180m and 232m to 270m for traverse line 1, 10m to 26m, 50m to 62m and 90m to 96m for traverse line 2, 44m to

78m and 82m to 96m for traverse line 3 and at distances 50m to 58m, 90m to 98m for traverse line 4.

- That the possible unplanned seepage pathway might, therefore, be defined to occur at an average elevation of 7m NDL and from distances 42m to 78m and 96m to 112m for traverse line 1, 50m to 62m and 90m to 96m for traverse line 2, 44m to 78m for traverse line 3 and exit between distance 90m to 98m for traverse line 4.
- That the induced polarization method was not able to clearly delineate potential seepage zones and pathways.

## 6.2 Recommendation

Further study is required to unravel the unplanned seepage conditions at the downstream end of the east dike using a combination of geophysical methods

Finally, drilling should be done to confirm the detected seepage zones and the delineated seepage pathway. The proposed drilling can be carried out to the inferred depth where the unplanned seepage water is predicted to rupture through the ground surface.

## REFERENCES

- Abdel Aal, G.Z., Ismail, A.M., Anderson, N.L., Atekwana, E.A., (2004). Geophysical Investigation of Seepage from an Earth fill Dam, Washington County, MO. *J. Appl. Geophys.* 44, 167–180.
- Aboelela, M.M., (2016). Control of Seepage through Earth Dams Based on Pervious Foundation Using Toe Drainage Systems 1158–1174.  
<https://doi.org/10.4236/jwarp.2016.812090>
- Acres International Limited, (1981). Kpong Hydroelectric Project- Geotechnical Completion Report. Niagara Falls, Canada.
- Alabi, A.A., Ogungbe, A.S., Adebo, B., Lamina, O., (2010). Induced Polarization Interpretation for Subsurface Characterisation : A case study of Obadore , Lagos State 1, 34–43.
- Bhattarai, S., Zhou, Y., Zhao, C., Yadav, R., (2016). An Overview on Types, Construction Method, Failure and Key Technical Issues During Construction of High Dams. *Electron. J. Geotech. Eng.* 21, 10415–10432.
- Blackett, F.L., (2013). Potential Failure Modes for Piping and Internal Erosion.
- Bureau of Reclamation, (2011). Embankment Dams 4.

- Burtman, V., Zhdanov, M.S., (2015). Induced Polarization Effect in Reservoir Rocks and its Modeling Based on Generalized Effective-Medium Theory. *Resour. Technol.* <https://doi.org/10.1016/j.reffit.2015.06.008>
- C. Nwokebuihe, S., M. Alotaibi, A., Elkrry, A., V. Torgashov, E., L. Anderson, N., (2017). Dam Seepage Investigation of an Earthfill Dam in Warren County, Missouri Using Geophysical Methods. *AIMS Geosci.* 3, 1–13. <https://doi.org/10.3934/geosci.2017.1.1>
- Carlsten, S., Johansson, S., Wörman, A., (1995). Radar Techniques for Indicating Internal Erosion in Embankment dams. *J. Appl. Geophys.* 33, 143–156. [https://doi.org/10.1016/0926-9851\(95\)90037-3](https://doi.org/10.1016/0926-9851(95)90037-3)
- Concepts, K., (2015). IV-4 . Internal Erosion Risks for Embankments and Foundations 1–134.
- Dams, E., (2011). Types of Dams Common to New Hampshire.
- Goodarzi, E., Shui, L.T., Ziaei, M., (2012). Dam Overtopping Risk using Probabilistic Concepts – Case study: The Meijaran Dam , Iran. *AIN SHAMS Eng. J.* <https://doi.org/10.1016/j.asej.2012.09.001>
- Herman, R., (2001). An Introduction to Electrical Resistivity in Geophysics. *Am. J. Phys.* 69, 943–952. <https://doi.org/10.1119/1.1378013>
- Icold, (2013). Bulletin 1XX - Internal Erosion of Existing Dams, Levees and Dikes, and their Foundations. Volume 1: *Internal erosion processes and engineering assessment (DRAFT, 22 January 2013)* 1, 151.
- Johansson, S., (1997). Seepage Monitoring in Embankment Dams.
- Jung, Y., Ha, H., Lee, Y., (2000). Application of Electrical Resistivity Imaging Techniques to Civil and Environmental Problems. *Geotech. Spec. Publ.* 296, 52–64.
- Kiplangat Vincent, K., Nicholas Muthama, M., Nicodemus Muoki, S., (2014). Darcy's Law Equation with Application to Underground Seepage in Earth Dams in Calculation of the Amount of Seepage. *Am. J. Appl. Math. Stat.* 2, 143–149. <https://doi.org/10.12691/ajams-2-3-8>
- Kirra, M.S., Zeidan, B.A., Shahien, M., Elshemy, M., (2015). Seepage Analysis of Walter F . George Dam , USA : A case Study. *Fac. Eng. Tanta Univ. Egypt* 6–9.
- Lin, C.P., Hung, Y.C., Yu, Z.H., Wu, P.L., (2013). Investigation of Abnormal Seepages in an Earth Dam Using Resistivity Tomography. *J. Geoengin.* 8, 61–70. [https://doi.org/10.6310/jog.2013.8\(2\).4](https://doi.org/10.6310/jog.2013.8(2).4)

- Moayed, R., Rashidian, V., Izadi, E., (2012). Evaluation of Phreatic Line in Homogeneous Earth Dams With Different Drainage System. 32nd Annu. USSD Conf. Innov. Dam Levee Des. Constr. Sustain. Water Manag.
- Murthy, G.S.R., Murty, K.G., Raghupathy, G., (2015). Designing Earth Dams Optimally. *Int. Ser. Oper. Res. Manag. Sci.* 212, 129–165. [https://doi.org/10.1007/978-1-4939-1007-6\\_7](https://doi.org/10.1007/978-1-4939-1007-6_7)
- New Hampshire Department of Environmental Services, (2011). Typical Failure Modes of Embankment Dams 2.
- Panthulu, T. V., Krishnaiah, C., Shirke, J.M., (2001). Detection of Seepage Paths in Earth Dams Using Self-Potential and Electrical Resistivity Methods. *Eng. Geol.* 59, 281–295. [https://doi.org/10.1016/S0013-7952\(00\)00082-X](https://doi.org/10.1016/S0013-7952(00)00082-X)
- Publication : USDA ARS [WWW Document], n.d. URL <https://www.ars.usda.gov/research/publications/publication/?seqNo115=250093> (accessed 11.9.17).
- Rajeeth, A., (2011). Failure of an Earth Dam: An Analysis of Earth Dam Break- Årbogen Dam, Nedre Eiker Municipality, Norway.
- Sachpazis, C.I., (2014). Experimental Conceptualisation of the Flow Net System Construction Inside the Body of Homogeneous Earth Embankment Dams. *Electron. J. Geotech. Eng.* 19 J, 2113–2136.
- Society, U.S., (1985). Materials for Embankment Dams Penman, A D M Int Water Power Dam ConstrV35, N1, Jan 1983, P15, *International Journal of Rock Mechanics and Mining Sciences* . [https://doi.org/10.1016/0148-9062\(85\)92801-3](https://doi.org/10.1016/0148-9062(85)92801-3)
- Spies, B.R., (1986). The Use and Misuse of Apparent Resistivity in Electromagnetic Methods. *Geophysics* 51, 1462. <https://doi.org/10.1190/1.1442194>
- Wehrmann, H., Johannes, H., (2006). Classification of Dams in Torrential Watersheds 829–838.
- Yan, Z.L., Wang, J.J., Chai, H.J., (2010). Influence of Water Level Fluctuation on Phreatic Line in Silty Soil Model Slope. *Eng. Geol.* 113, 90–98. <https://doi.org/10.1016/j.enggeo.2010.02.004>

# APPENDICES

## Appendix A Edited data for 50 data points for Resistivity and Chargeability

### Traverse line 1

Project10	GradientPlus_1										
	2										
11											
15											
Type	of	measurment	(0=app.	resistivity	1=resistance)						
0											
1098											
2											
1											
Chargeability											
msec.											
0.15	1.1										
4	0	0	20	0	2	0	4	0	2630.192	26.3821	
4	2	0	22	0	4	0	6	0	1634.446	19.606	
4	4	0	24	0	6	0	8	0	1201.333	146.0665	
4	6	0	26	0	8	0	10	0	1404.713	22.5965	
4	10	0	30	0	12	0	14	0	1691.498	0.9813	
4	0	0	20	0	16	0	18	0	1935.358	6.6161	
4	2	0	22	0	18	0	20	0	1380.14	64.314	
4	4	0	24	0	20	0	22	0	1023.963	8.5034	
4	6	0	26	0	22	0	24	0	1161.917	162.2711	
4	22	0	42	0	24	0	26	0	892.0604	31.7805	
4	12	0	32	0	28	0	30	0	1083.898	151.5679	
4	24	0	44	0	26	0	28	0	1160.67	79.3627	

4	14	0	34	0	30	0	32	0	1808.151	16.48
4	28	0	48	0	30	0	32	0	1239.014	11.443
4	18	0	38	0	34	0	36	0	1326.335	3.2825
4	20	0	40	0	36	0	38	0	1119.681	157.2999
4	32	0	52	0	34	0	36	0	1899.732	31.9357
4	22	0	42	0	38	0	40	0	1826.734	14.1886
4	36	0	56	0	38	0	40	0	1400.84	57.3597
4	26	0	46	0	42	0	44	0	1539.386	25.2789
4	38	0	58	0	40	0	42	0	958.41	380.843
4	28	0	48	0	44	0	46	0	866.7487	14.0788
4	32	0	52	0	48	0	50	0	888.6492	10.8368
4	44	0	64	0	46	0	48	0	1128.103	96.9541
4	46	0	66	0	48	0	50	0	938.8913	6.0131
4	36	0	56	0	52	0	54	0	1061.503	2.5825
4	50	0	70	0	52	0	54	0	782.3915	5.2849
4	40	0	60	0	56	0	58	0	1284.947	4.478
4	42	0	62	0	58	0	60	0	1025.919	27.242
4	54	0	74	0	56	0	58	0	1015.191	5.8162
4	44	0	64	0	60	0	62	0	1105.811	20.1409
4	46	0	66	0	62	0	64	0	1437.933	72.8015
4	48	0	68	0	64	0	66	0	1652.97	1.1473
4	60	0	80	0	62	0	64	0	1118.617	16.171
4	50	0	70	0	66	0	68	0	1328.425	26.2056
4	62	0	82	0	64	0	66	0	911.814	91.3942
4	64	0	84	0	66	0	68	0	1134.725	214.1211
4	54	0	74	0	70	0	72	0	1704.046	8.8936
4	56	0	76	0	72	0	74	0	2102.525	6.2112

4	68	0	88	0	70	0	72	0	1199.773	25.8791
4	60	0	80	0	76	0	78	0	1751.627	20.3945
4	72	0	92	0	74	0	76	0	1814.656	37.7728
4	62	0	82	0	78	0	80	0	1848.685	24.7308
4	76	0	96	0	78	0	80	0	1455.163	100.7642
4	66	0	86	0	82	0	84	0	1570.909	92.7077
4	78	0	98	0	80	0	82	0	998.7925	383.4824
4	68	0	88	0	84	0	86	0	918.7979	12.162
4	72	0	92	0	88	0	90	0	905.0232	7.6908
4	84	0	104	0	86	0	88	0	914.7679	310.5796

**Traverse line 2**

Project60	GradientPlus_3									
	2									
11										
15										
Type	of	resistivity	data	(1=resista	n0=resistivity)					
0										
1527										
2										
1										
Chargeability										
msec.										
	0.15	1.1								
4	0	0	20	0	2	0	4	0	123.6439	8.5289
4	2	0	22	0	4	0	6	0	397.5329	1.8134
4	4	0	24	0	6	0	8	0	397.7896	1.5037

4	6	0	26	0	8	0	10	0	521.0229	3.3597
4	8	0	28	0	10	0	12	0	206.1663	9.9808
4	10	0	30	0	12	0	14	0	731.741	2.0911
4	0	0	20	0	16	0	18	0	52.2422	6.9113
4	12	0	32	0	14	0	16	0	438.9766	0.9419
4	2	0	22	0	18	0	20	0	251.7314	1.8986
4	4	0	24	0	20	0	22	0	600.147	0.4266
4	16	0	36	0	18	0	20	0	136.7451	2.5541
4	6	0	26	0	22	0	24	0	426.2853	2.401
4	18	0	38	0	20	0	22	0	50.5593	4.0005
4	8	0	28	0	24	0	26	0	305.8641	4.276
4	20	0	40	0	22	0	24	0	223.6799	3.3369
4	10	0	30	0	26	0	28	0	62.1859	4.2975
4	22	0	42	0	24	0	26	0	577.7721	2.9641
4	12	0	32	0	28	0	30	0	296.8261	4.9767
4	24	0	44	0	26	0	28	0	432.7483	1.5647
4	14	0	34	0	30	0	32	0	44.9088	17.7941
4	26	0	46	0	28	0	30	0	306.1209	12.1952
4	16	0	36	0	32	0	34	0	240.4474	540.9556
4	28	0	48	0	30	0	32	0	49.8506	103.101
4	18	0	38	0	34	0	36	0	91.8028	901
4	30	0	50	0	32	0	34	0	117.8897	216.8598
4	20	0	40	0	36	0	38	0	100.0103	901
4	32	0	52	0	34	0	36	0	10.5985	59.6343
4	22	0	42	0	38	0	40	0	208.9083	901
4	34	0	54	0	36	0	38	0	24.553	901
4	24	0	44	0	40	0	42	0	126.3695	236.8931

4	36	0	56	0	38	0	40	0	114.1031	112.9377
4	26	0	46	0	42	0	44	0	37.485	369.2216
4	28	0	48	0	44	0	46	0	133.5138	342.1229
4	40	0	60	0	42	0	44	0	217.3112	901
4	30	0	50	0	46	0	48	0	51.6494	778.7447
4	42	0	62	0	44	0	46	0	76.156	639.6404
4	32	0	52	0	48	0	50	0	160.7584	91.1914
4	44	0	64	0	46	0	48	0	64.0312	32.972
4	34	0	54	0	50	0	52	0	299.0587	13.591
4	46	0	66	0	48	0	50	0	31.8646	260.6858
4	36	0	56	0	52	0	54	0	295.1266	144.2701
4	48	0	68	0	50	0	52	0	84.802	255.0875
4	38	0	58	0	54	0	56	0	174.9338	311.2411
4	50	0	70	0	52	0	54	0	77.6618	123.5893
4	40	0	60	0	56	0	58	0	198.0565	97.6437
4	52	0	72	0	54	0	56	0	56.0112	73.3556
4	42	0	62	0	58	0	60	0	378.7917	34.8688
4	54	0	74	0	56	0	58	0	100.1294	118.4709
4	44	0	64	0	60	0	62	0	276.383	0.3818

**Traverse line 3**

Project60	GradientPlus_1									
	2									
11										
15										
Type	of	resistivity	data	(1=resista	n0=resistivity)					
0										

1677											
2											
1											
Chargeability											
msec.											
	0.15	1.1									
4	0	0	20	0	2	0	4	0	2001.586	25.5578	
4	2	0	22	0	4	0	6	0	5158.07	39.7878	
4	4	0	24	0	6	0	8	0	6275.447	26.4621	
4	2	0	22	0	18	0	20	0	8280.999	23.0131	
4	4	0	24	0	20	0	22	0	2311.15	30.0404	
4	16	0	36	0	18	0	20	0	1967.823	31.3661	
4	6	0	26	0	22	0	24	0	1229.846	44.5161	
4	18	0	38	0	20	0	22	0	3147.236	13.4181	
4	8	0	28	0	24	0	26	0	681.1834	632.0974	
4	20	0	40	0	22	0	24	0	6852.402	417.3539	
4	10	0	30	0	26	0	28	0	2169.395	530.2632	
4	22	0	42	0	24	0	26	0	755.6492	597.8932	
4	12	0	32	0	28	0	30	0	6761.925	6.801	
4	24	0	44	0	26	0	28	0	123.013	901	
4	14	0	34	0	30	0	32	0	32.2554	901	
4	26	0	46	0	28	0	30	0	176.5037	544.1943	
4	16	0	36	0	32	0	34	0	1026.929	311.4184	
4	28	0	48	0	30	0	32	0	1254.483	901	
4	18	0	38	0	34	0	36	0	1895.113	679.2959	
4	20	0	40	0	36	0	38	0	1941.254	106.7523	
4	32	0	52	0	34	0	36	0	362.4079	102.9033	

4	22	0	42	0	38	0	40	0	2131.502	479.532
4	34	0	54	0	36	0	38	0	1195.47	262.1985
4	36	0	56	0	38	0	40	0	1990.472	24.5543
4	38	0	58	0	40	0	42	0	1681.896	44.1655
4	28	0	48	0	44	0	46	0	8461.687	37.6036
4	40	0	60	0	42	0	44	0	1627.147	0.7394
4	42	0	62	0	44	0	46	0	7825.48	11.9639
4	46	0	66	0	48	0	50	0	620.7809	2.8839
4	36	0	56	0	52	0	54	0	5471.93	17.5703
4	48	0	68	0	50	0	52	0	311.8258	17.6957
4	38	0	58	0	54	0	56	0	4457.185	18.4563
4	50	0	70	0	52	0	54	0	579.139	19.6575
4	40	0	60	0	56	0	58	0	133.4813	10.7133
4	52	0	72	0	54	0	56	0	7409.624	32.798
4	42	0	62	0	58	0	60	0	117.9572	20.818
4	54	0	74	0	56	0	58	0	4521.155	17.868
4	44	0	64	0	60	0	62	0	97.2701	0.2215
4	56	0	76	0	58	0	60	0	148.8011	1.002
4	58	0	78	0	60	0	62	0	139.6394	0.1477
4	48	0	68	0	64	0	66	0	1434.48	568.0892
4	60	0	80	0	62	0	64	0	112.8362	458.4454
4	50	0	70	0	66	0	68	0	252.7242	91.2438
4	62	0	82	0	64	0	66	0	105.5547	65.2962
4	64	0	84	0	66	0	68	0	100.1064	127.6093
4	54	0	74	0	70	0	72	0	1653.774	102.6241
4	66	0	86	0	68	0	70	0	114.1183	30.2941
4	56	0	76	0	72	0	74	0	1439.552	2.9346

4	68	0	88	0	70	0	72	0	244.9725	3.483
---	----	---	----	---	----	---	----	---	----------	-------

### Traverse line 4

Project9	GradientPlus_1									
	2									
11										
15										
Type	of	resistivity	data	(1=resistance, 0=resistivity)						
0										
1795										
2										
1										
Chargeability										
msec.										
	0.15	1.1								
4	0	0	20	0	2	0	4	0	102.351	12.8649
4	2	0	22	0	4	0	6	0	98.2952	0.9681
4	4	0	24	0	6	0	8	0	107.2207	0.6989
4	6	0	26	0	8	0	10	0	113.2861	0.8451
4	8	0	28	0	10	0	12	0	83.1697	0.4006
4	10	0	30	0	12	0	14	0	23.3965	10.8959
4	0	0	20	0	16	0	18	0	31.833	6.6839
4	2	0	22	0	18	0	20	0	24.8692	1.3945
4	14	0	34	0	16	0	18	0	44.8416	0.565
4	4	0	24	0	20	0	22	0	32.8034	0.5159
4	16	0	36	0	18	0	20	0	34.7753	0.5045
4	6	0	26	0	22	0	24	0	32.3571	0.7914
4	18	0	38	0	20	0	22	0	33.4807	0.3944

4	8	0	28	0	24	0	26	0	41.3274	1.1965
4	20	0	40	0	22	0	24	0	25.8635	1.6288
4	10	0	30	0	26	0	28	0	38.6169	0.7165
4	22	0	42	0	24	0	26	0	31.4305	0.5413
4	24	0	44	0	26	0	28	0	31.5095	0.0215
4	14	0	34	0	30	0	32	0	28.8561	0.5204
4	26	0	46	0	28	0	30	0	42.1138	0.5083
4	16	0	36	0	32	0	34	0	21.4928	0.3857
4	28	0	48	0	30	0	32	0	43.3184	0.6108
4	18	0	38	0	34	0	36	0	25.5072	0.9518
4	30	0	50	0	32	0	34	0	39.967	0.9267
4	20	0	40	0	36	0	38	0	31.5411	2.6885
4	32	0	52	0	34	0	36	0	27.3074	4.3807
4	22	0	42	0	38	0	40	0	33.6675	1.7029
4	34	0	54	0	36	0	38	0	21.332	1.0507
4	24	0	44	0	40	0	42	0	33.2394	0.6613
4	36	0	56	0	38	0	40	0	23.2129	3.1477
4	26	0	46	0	42	0	44	0	37.2184	2.0905
4	38	0	58	0	40	0	42	0	34.9056	1.47
4	28	0	48	0	44	0	46	0	31.3694	0.3358
4	40	0	60	0	42	0	44	0	35.0081	11.5756
4	30	0	50	0	46	0	48	0	27.4906	0.4047
4	42	0	62	0	44	0	46	0	26.8379	1.9444
4	32	0	52	0	48	0	50	0	41.5917	2.0138
4	44	0	64	0	46	0	48	0	28.6597	5.6118
4	34	0	54	0	50	0	52	0	41.9539	3.2619
4	46	0	66	0	48	0	50	0	33.3932	0.8982

4	36	0	56	0	52	0	54	0	42.6224	1.2023
4	48	0	68	0	50	0	52	0	27.6266	0.6982
4	38	0	58	0	54	0	56	0	53.8356	1.2696
4	50	0	70	0	52	0	54	0	27.0265	8.2448
4	40	0	60	0	56	0	58	0	57.8892	0.8748
4	52	0	72	0	54	0	56	0	47.0544	7.8316
4	42	0	62	0	58	0	60	0	48.5463	4.46
4	54	0	74	0	56	0	58	0	43.2917	0.2444
4	44	0	64	0	60	0	62	0	46.7392	2.759

### Appendix B Software Used

- RES2DINV
- ArcGIS
- Microsoft Word 2010
- Microsoft Excel 2010



## Appendix C Overburden soil stratigraphy of East Dike

